Dyfuzja gazów szlachetnych w nanoporach materiałów węglowych

Piotr A. Gauden[1], Sylwester Furmaniak[1], Wojciech Zieliński[1], Piotr Kowalczyk[2]

[1] Faculty of Chemistry, Physicochemistry of Carbon Materials Research Group, Nicolaus Copernicus University in Toruń, Gagarin St. 7, 87–100 Toruń, Poland

[2] School of Engineering and Information Technology, Murdoch University, Murdoch, Western Australia 6150, Australia

e-mail: gaudi@umk.pl

KONFERENCJĘ UŻYTKOWNIKÓW KDM 2017
„Nowe trendy w użytkowaniu KDM”

[MOLECULAR FORMS]

THE MOTHER OF ALL GRAPHITES

Graphene (*below, top*), a plane of carbon atoms that resembles chicken wire, is the basic building block of all the "graphitic" materials depicted below. Graphite (*bottom row at left*), the main component of pencil "lead," is a crumbly substance that resembles a layer cake of weakly bonded graphene sheets. When graphene is wrapped into rounded forms, fullerenes result. They include honeycombed cylinders known as carbon nanotubes (*bottom row at center*) and soccer ball–shaped molecules called buckyballs (*bottom row at right*), as well as various shapes that combine the two forms.

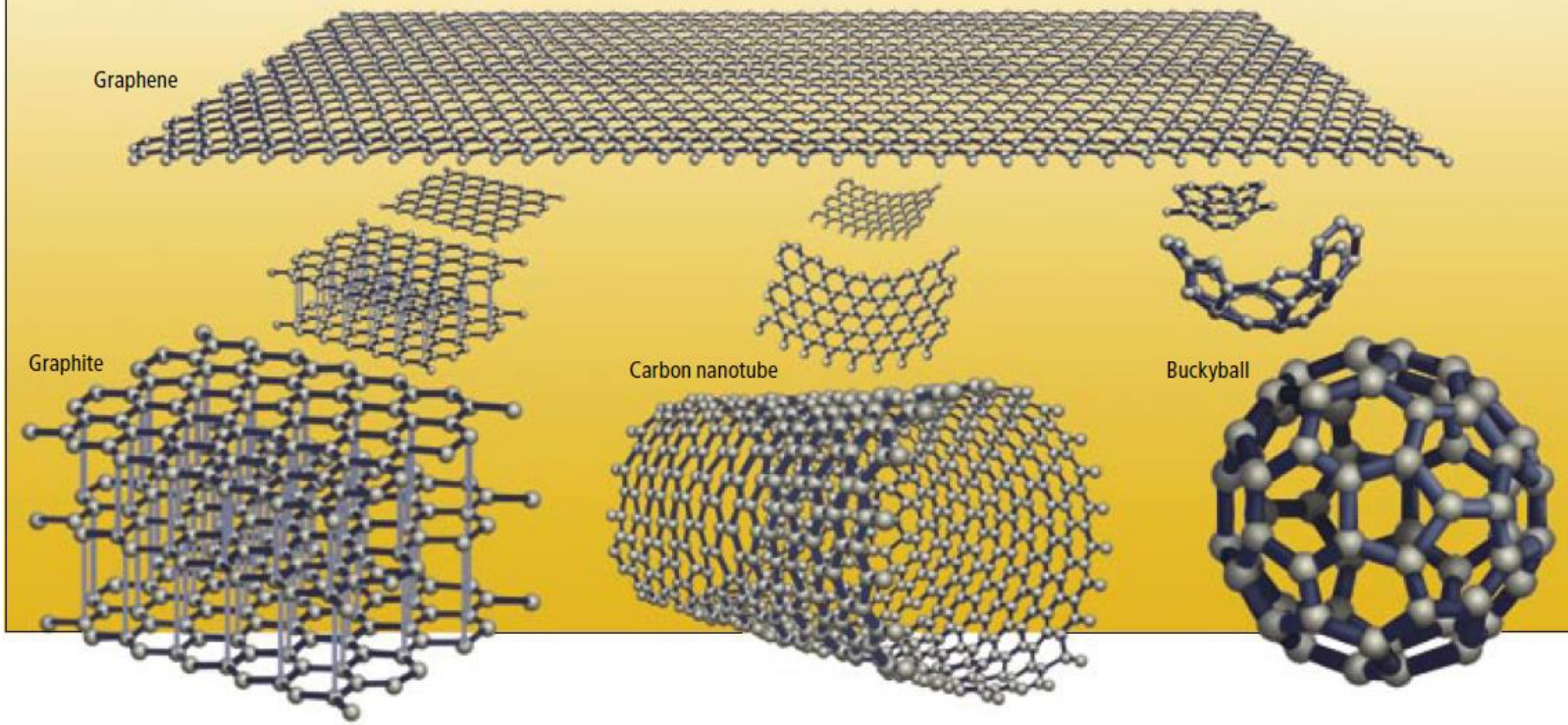

CARBON 50 (2012) 741–747

Available at www.sciencedirect.com

SciVerse ScienceDirect

journal homepage: www.elsevier.com/locate/carbon

Guest Editorial

Nomenclature of sp^2 carbon nanoforms

Irene Suarez-Martinez
Institute des Matériaux Jean Rouxel, CNRS,
Université de Nantes, BP 32229, 44322 Nantes, France
Nanochemistry Research Institute, Curtin University,
GPO Box U1987, Perth 6845, Australia
E-mail address: i.suarez-martinez@curtin.edu.au

Nicole Grobert
Department of Materials, University of Oxford,
Oxford OX1 3PH, UK
E-mail address: nicole.grobert@materials.ox.ac.uk

Christopher P. Ewels
Institute des Matériaux Jean Rouxel, CNRS,
Université de Nantes, BP 32229, 44322 Nantes, France
E-mail address: chris.ewels@cnrs-imn.fr

0008-6223/$ - see front matter

doi:10.1016/j.carbon.2011.11.002

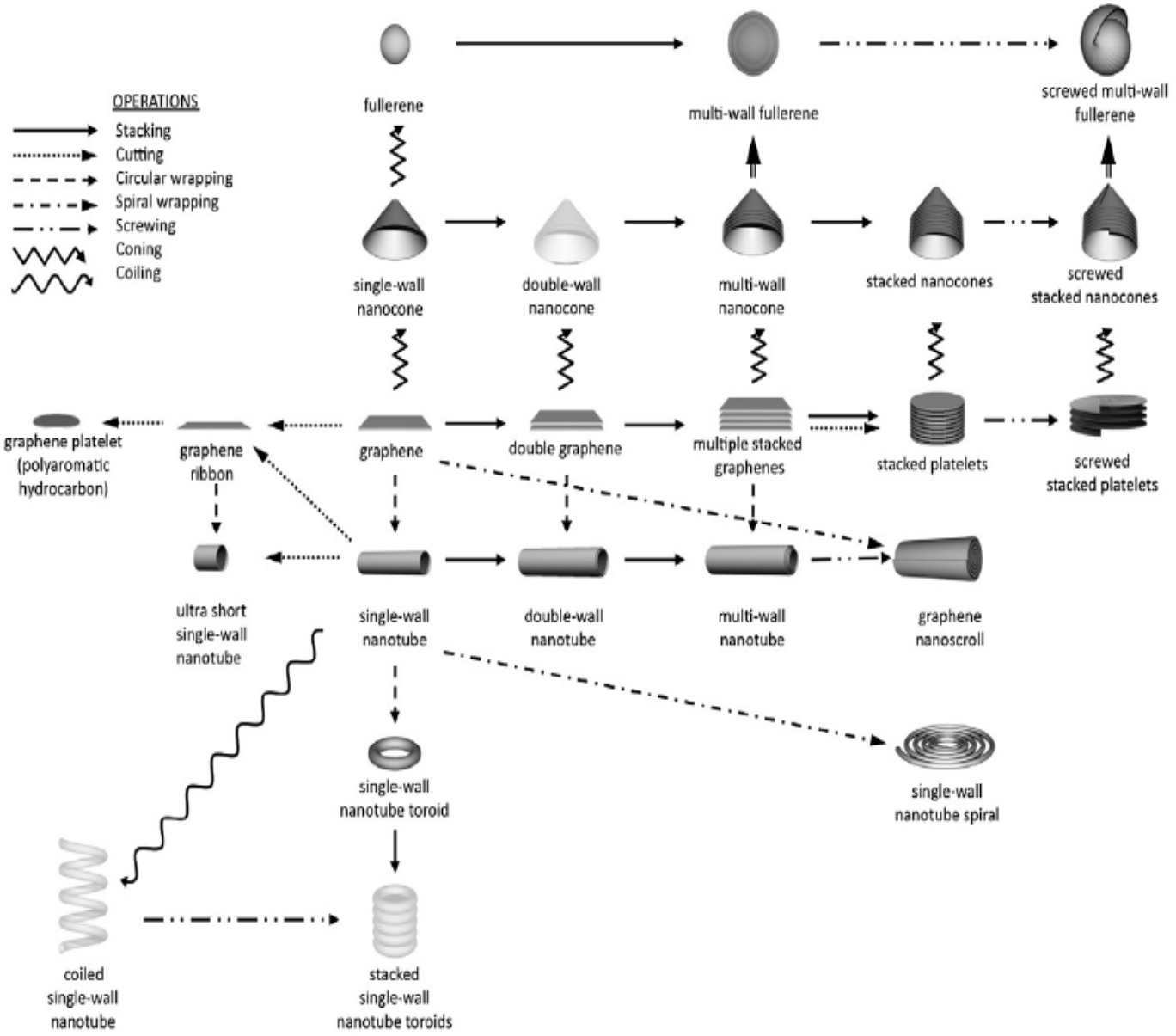

Fig. 2 – "Family tree" of primary carbon nanoforms showing the topological relationships between them. We note that all 1D forms can undergo the same operations as for the single-walled nanotube. For each form further operations are also possible such as polygonisation (see text). In addition hybrid forms (such as fullerene-filled nanotubes) are not included. Forms which have not been identified experimentally are faded. A description of each operation can be found in the text.

OMC

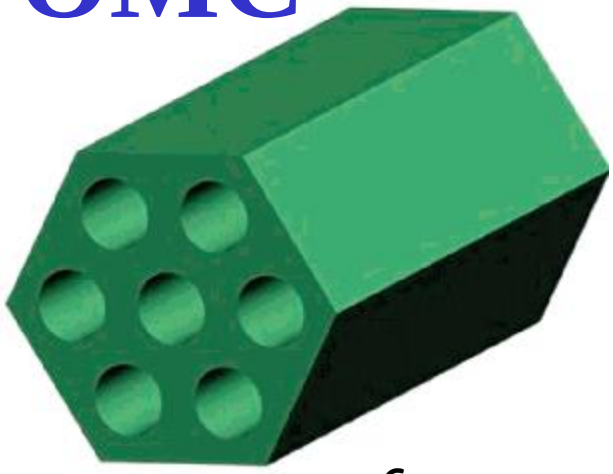

p6mm

SBA-15

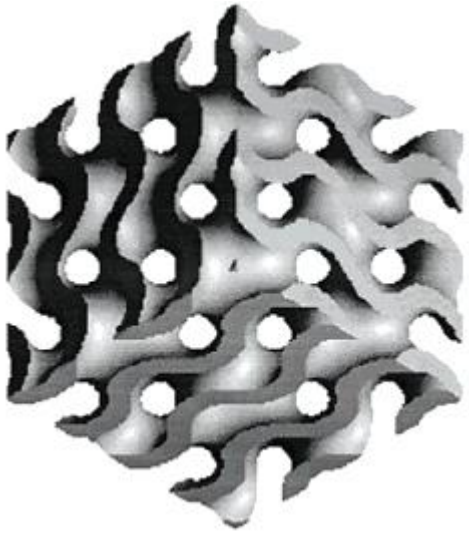

Ia3d,

MCM-48

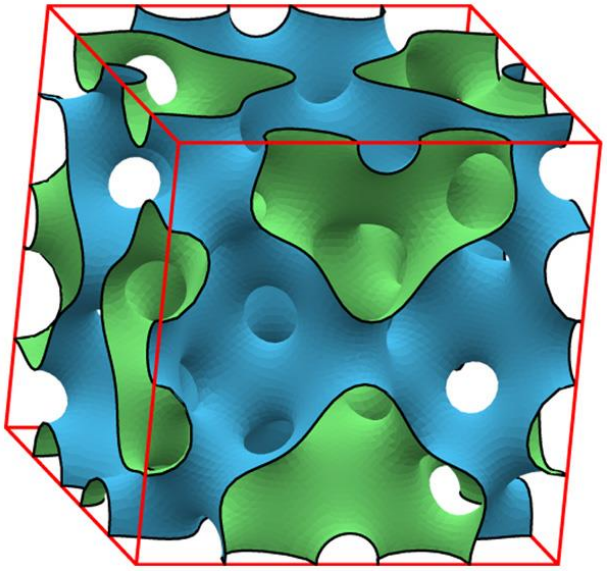

Pm3n

SBA-1 and 6

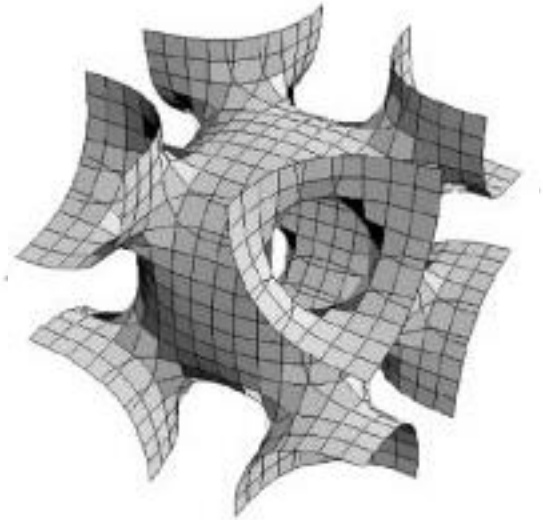

Im3m

SBA-16

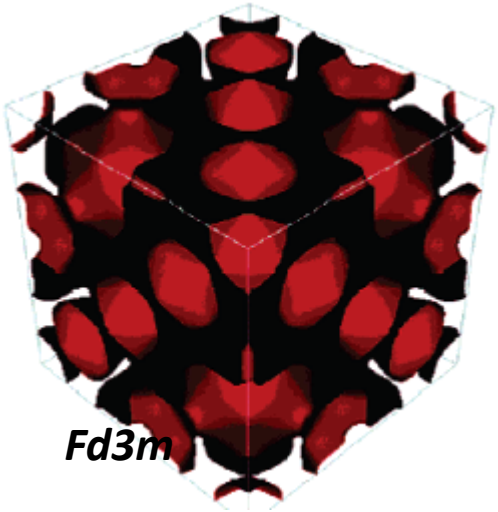

Fd3m

FDU-2

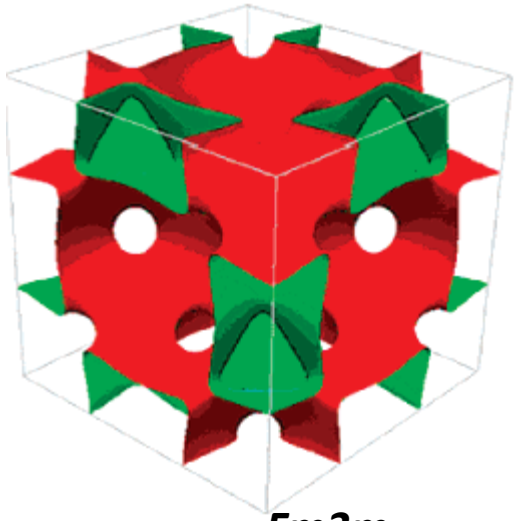

Fm3m.

KIT-5

Hydrogen storage in nanoporous carbon materials: myth and facts

Piotr Kowalczyk,[a] Robert Hołyst,[a] Mauricio Terrones[b] and Humberto Terrones[b]

Received 22nd December 2006, Accepted 9th March 2007
First published as an Advance Article on the web 23rd March 2007
DOI: 10.1039/b618747a

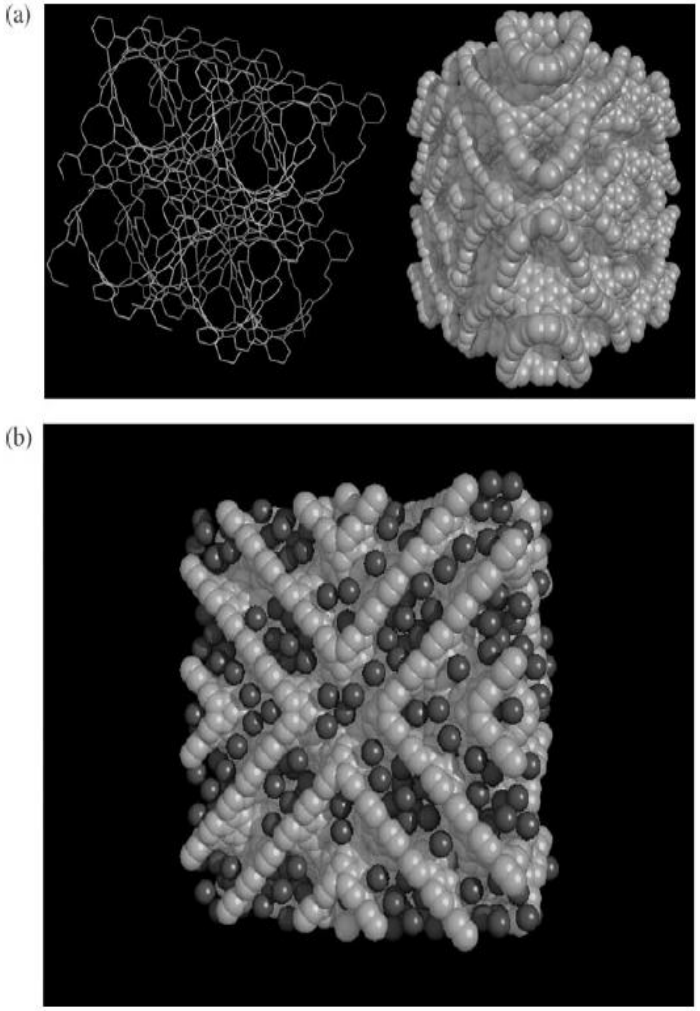

Fig. 5 (a) Diamond carbon nanoporous material. Left image shows carbon rings on the surface and right image shows eight unit cells of the structure decorated by carbon atoms. (b) A snapshot of hydrogen adsorbed in the diamond nanoporous carbon material at 3.8 MPa and 77 K collected from the simulation (cross-section is shown).

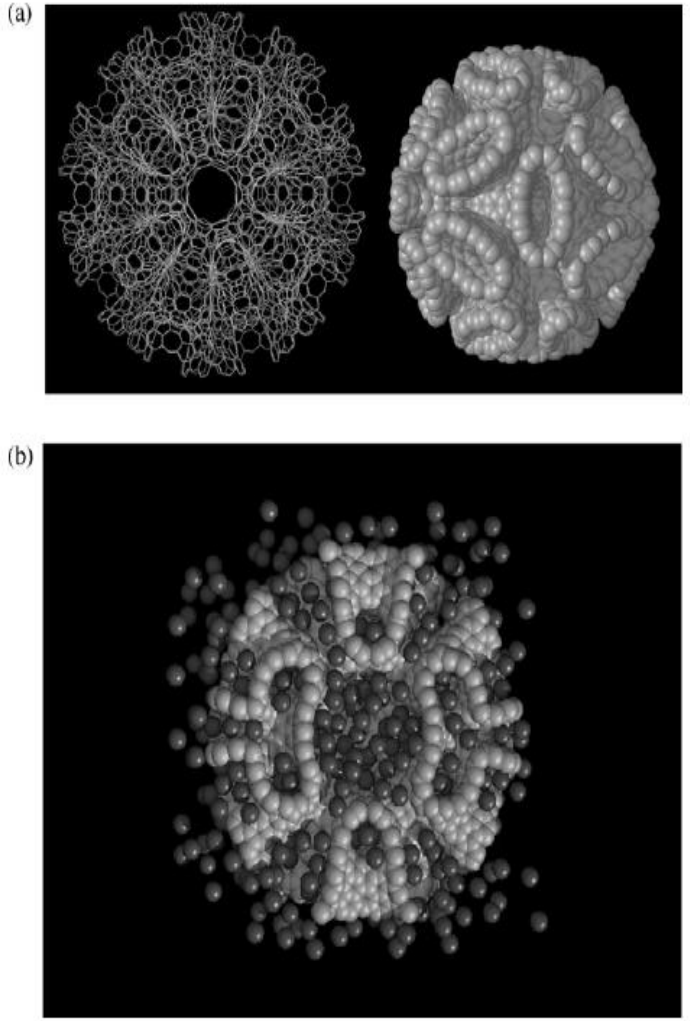

Fig. 4 (a) The quasi-periodic icosahedral nanoporous carbon material. Left figure shows carbon rings on the surface and right figure shows eight unit cells of the structure decorated by carbon atoms. (b) A snapshot of hydrogen adsorbed in the quasi-periodic icosahedral nanoporous carbon material at 3.8 MPa and 77 K.

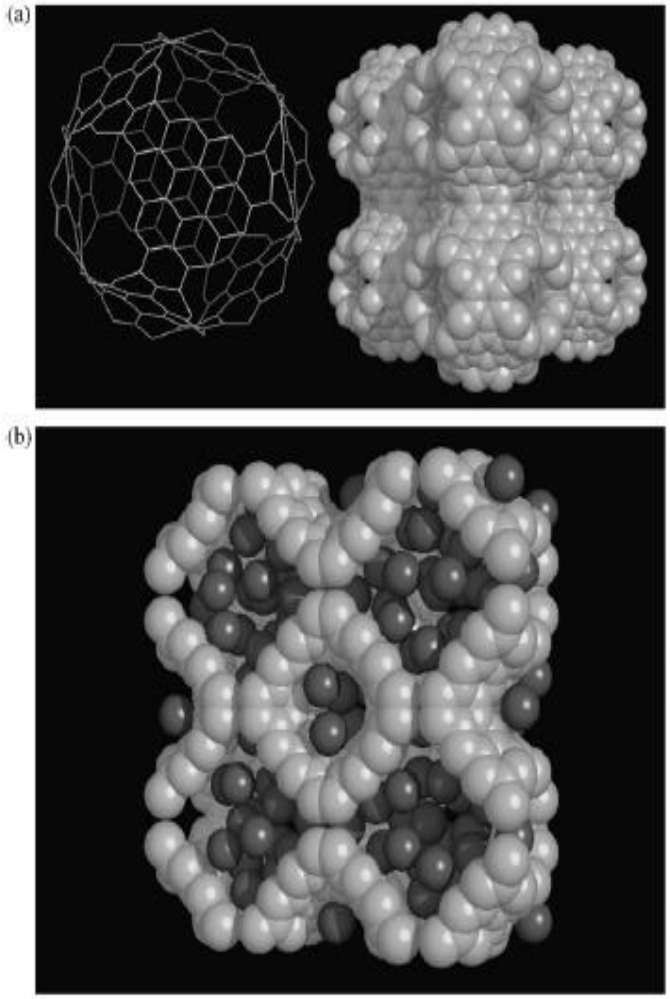

Fig. 6 (a) Primitive carbon nanoporous material. Left image shows carbon rings on the surface and right image shows eight unit cells of the structure decorated by carbon atoms. (b) A snapshot of hydrogen adsorbed in the primitive nanoporous carbon material at 3.8 MPa and 77 K collected from the simulation (cross section is shown).

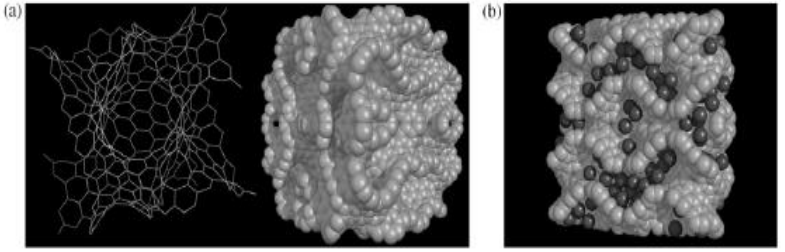

Fig. 7 (a) Gyroid carbon nanoporous material. Left image shows carbon rings on the surface and right image shows eight unit cells of the structure decorated by carbon atoms. (b) A snapshot of hydrogen adsorbed in the gyroid nanoporous carbon material at 3.8 MPa and 77 K collected from the FH-GCMC simulation (cross section of the material).

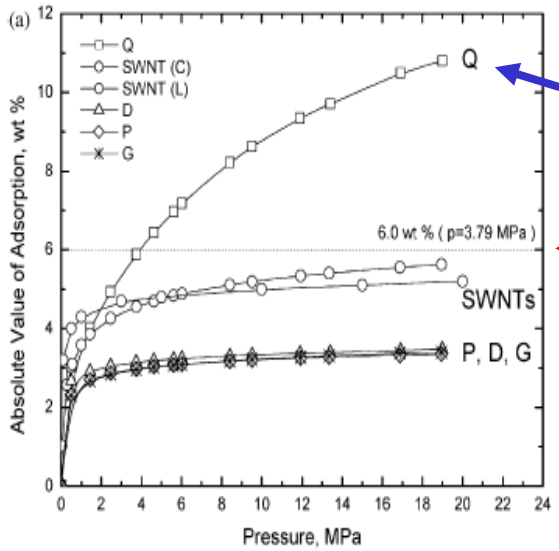

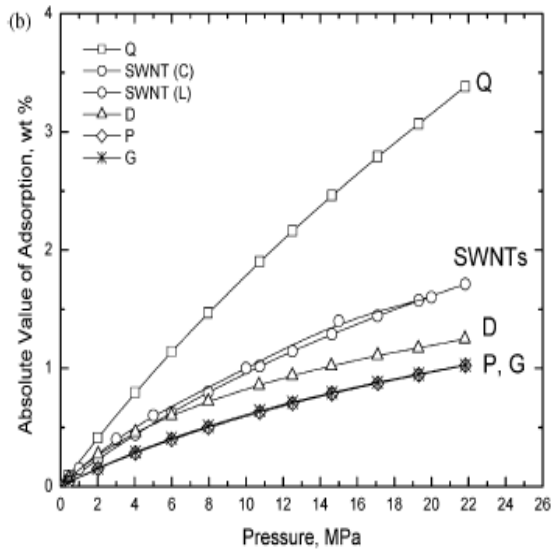

Fig. 1 (a) Simulated absolute value of adsorption (hydrogen gravimetric weight percent) at 77 K from the computer simulations. Abbreviations: Q – quasi-periodic icosahedral nanoporous carbon material, SWNT (C) – hexagonal bundle of SWNTs, SWNT (L) – simulation results of hydrogen storage in SWNTs (single wall carbon nanotubes) taken from Levesque *et al.*[16] for comparison with our results, D – diamond nanoporous carbon material, P – primitive nanoporous carbon material, and G – gyroid nanoporous carbon material. (b) Same at 303 K.

Periodic Table of the Elements

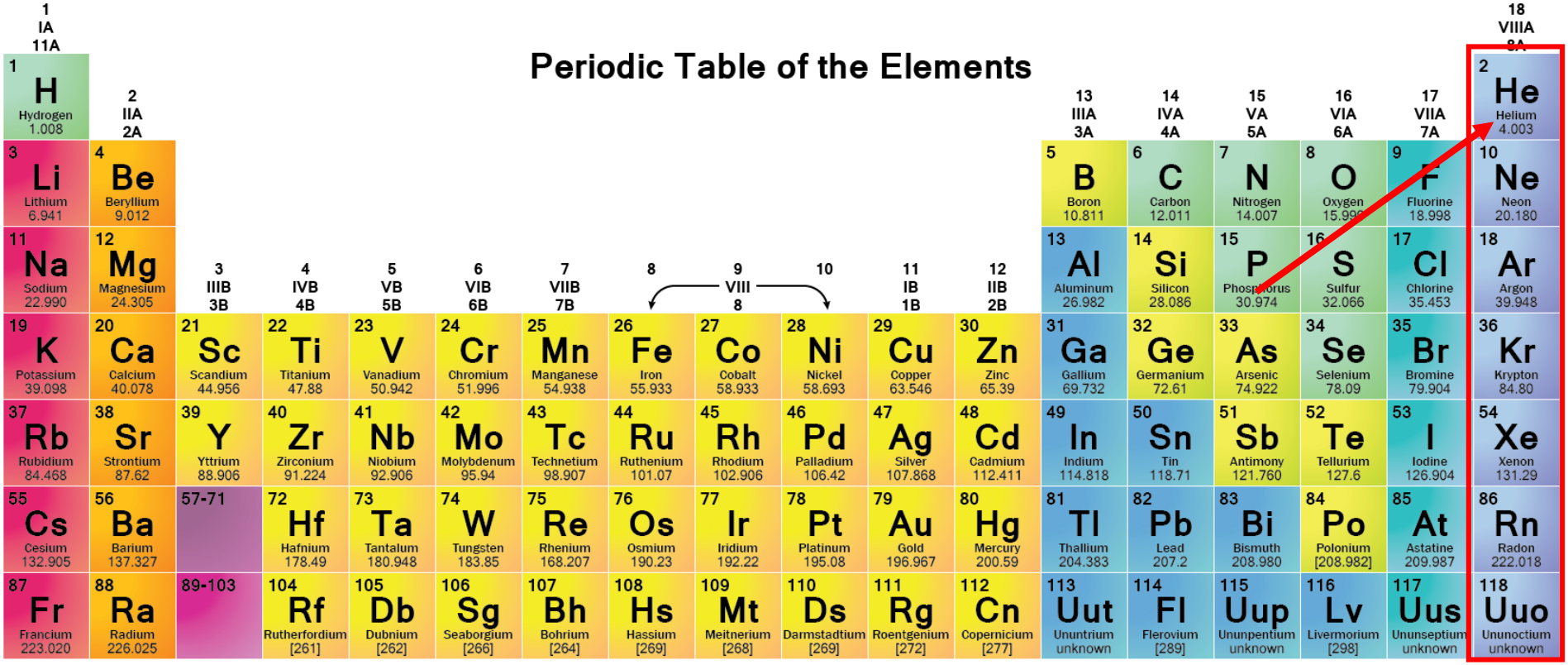

Lanthanide Series	57 La Lanthanum 138.906	58 Ce Cerium 140.115	59 Pr Praseodymium 140.908	60 Nd Neodymium 144.24	61 Pm Promethium 144.913	62 Sm Samarium 150.36	63 Eu Europium 151.966	64 Gd Gadolinium 157.25	65 Tb Terbium 158.925	66 Dy Dysprosium 162.50	67 Ho Holmium 164.930	68 Er Erbium 167.26	69 Tm Thulium 168.934	70 Yb Ytterbium 173.04	71 Lu Lutetium 174.967
Actinide Series	89 Ac Actinium 227.028	90 Th Thorium 232.038	91 Pa Protactinium 231.036	92 U Uranium 238.029	93 Np Neptunium 237.048	94 Pu Plutonium 244.064	95 Am Americium 243.061	96 Cm Curium 247.070	97 Bk Berkelium 247.070	98 Cf Californium 251.080	99 Es Einsteinium [254]	100 Fm Fermium 257.095	101 Md Mendelevium 258.1	102 No Nobelium 259.101	103 Lr Lawrencium [262]

Alkali Metal | Alkaline Earth | Transition Metal | Semimetal | Nonmetal | Basic Metal | Halogen | Noble Gas | Lanthanide | Actinide

Why noble gases… ?

Helium is a rare gas with a wide range of applications
(e.g., lasers, fluorescent light fixtures, medical imaging, cooling technologies, nuclear physics, diving technologies, and others).

Why noble gases… ?

Helium is a rare gas with a wide range of applications
(e.g., lasers, fluorescent light fixtures, medical imaging, cooling technologies, nuclear physics, diving technologies, and others).

Industrial technologies currently being used for purification include combined cryogenic distillation and **adsorption technologies** (e.g., pressure-swing adsorption, vacuum pressure swing adsorption, and temperature swing adsorption).

Why noble gases… ?

Helium is a rare gas with a wide range of applications
(e.g., lasers, fluorescent light fixtures, medical imaging, cooling technologies, nuclear physics, diving technologies, and others).

Industrial technologies currently being used for purification include combined cryogenic distillation and **adsorption technologies** (e.g., pressure-swing adsorption, vacuum pressure swing adsorption, and temperature swing adsorption).

Similarly, resources of He (e.g., natural gas, air, and waste gases of ammonia synthesis) **are composed of various small particles** (such as CH_4, CO, Ar, Ne, O_2, and others) **that need to be removed through purification processes**.

Why noble gases… ?

Helium is a rare gas with a wide range of applications
(e.g., lasers, fluorescent light fixtures, medical imaging, cooling technologies, nuclear physics, diving technologies, and others).

Industrial technologies currently being used for purification include combined cryogenic distillation and **adsorption technologies** (e.g., pressure-swing adsorption, vacuum pressure swing adsorption, and temperature swing adsorption).

Similarly, resources of He (e.g., natural gas, air, and waste gases of ammonia synthesis) **are composed of various small particles** (such as CH_4, CO, Ar, Ne, O_2, and others) **that need to be removed through purification processes**.

Separation of fluid mixtures consisting of light particles (such as He and H_2) is a far more challenging problem. This is because the surface forces (i.e., short range London dispersion interaction between light particles and solid atoms) are very weak.

Why noble gases… ?

Helium is a rare gas with a wide range of applications
(e.g., lasers, fluorescent light fixtures, medical imaging, cooling technologies, nuclear physics, diving technologies, and others).

Industrial technologies currently being used for purification include combined cryogenic distillation and **adsorption technologies** (e.g., pressure-swing adsorption, vacuum pressure swing adsorption, and temperature swing adsorption).

Similarly, resources of He (e.g., natural gas, air, and waste gases of ammonia synthesis) **are composed of various small particles** (such as CH_4, CO, Ar, Ne, O_2, and others) **that need to be removed through purification processes**.

Separation of fluid mixtures consisting of light particles (such as He and H_2) is a far more challenging problem. This is because the surface forces (i.e., short range London dispersion interaction between light particles and solid atoms) are very weak.

Due to the small size of He atoms, the **diffusion rate** through materials **is a very fast process**.

Why noble gases… ?

Helium is a rare gas with a wide range of applications
(e.g., lasers, fluorescent light fixtures, medical imaging, cooling technologies, nuclear physics, diving technologies, and others).

Industrial technologies currently being used for purification include combined cryogenic distillation and **adsorption technologies** (e.g., pressure-swing adsorption, vacuum pressure swing adsorption, and temperature swing adsorption).

Similarly, resources of He (e.g., natural gas, air, and waste gases of ammonia synthesis) **are composed of various small particles** (such as CH_4, CO, Ar, Ne, O_2, and others) **that need to be removed through purification processes**.

Separation of fluid mixtures consisting of light particles (such as He and H_2) is a far more challenging problem. This is because the surface forces (i.e., short range London dispersion interaction between light particles and solid atoms) are very weak.

Due to the small size of He atoms, the **diffusion rate** through materials **is a very fast process**.

The main aim: looking for new carbon materials!

THE JOURNAL OF PHYSICAL CHEMISTRY C

Article

pubs.acs.org/JPCC

Exotic Cubic Carbon Allotropes

Meng Hu,[†] Fei Tian,[‡] Zhisheng Zhao,[†] Quan Huang,[†] Bo Xu,[†] Li-Min Wang,[†] Hui-Tian Wang,[‡] Yongjun Tian,[†] and Julong He*[,†]

[†]State Key Laboratory of Metastable Materials Science and Technology, Yanshan University, Qinhuangdao 066004, China

[‡]School of Physics and Key Laboratory of Weak-Light Nonlinear Photonics, Ministry of Education, Nankai University, Tianjin 300071, China

ABSTRACT: Elemental carbon exists in various aesthetically pleasing architectures. These forms include a group of synthesized allotropes with cubic modifications that have taken controversial or even unidentified crystal structures, which makes determining their physical properties difficult. In this study, four novel cubic carbon polymorphs (fcc-C_{10}, fcc-C_{12}, bcc-C_{20}, and fcc-C_{32}) that exhibit lattice parameters within the same range as those of undetermined cubic carbon allotropes are proposed by employing a newly developed ab initio particle-swarm optimization methodology for crystal structure prediction. The four structures are all three-dimensional polymers consisting of unique, small C_{10}, C_{12}, C_{20}, and C_{32} cages with quite low density. Investigation of their electronic and mechanical properties illustrate that the cage-like cubic carbons are all semiconductors with excellent mechanical performance, specifically superhardness and high ductility. Moreover, we readily explain a long-standing controversial experimentally synthesized cubic carbon (viz., the so-called "superdense" carbon) using the previously proposed bcc C_6 based on the coincident lattice constant and electron diffraction data between the theoretical and experimental results.

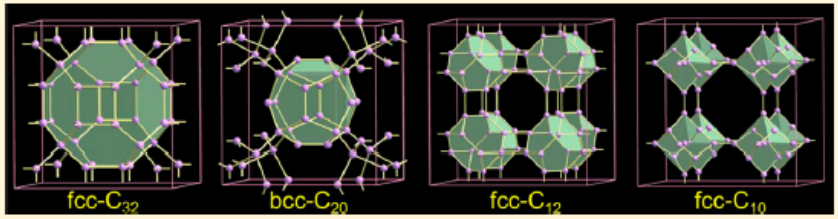

dx.doi.org/10.1021/jp3064323 | J. Phys. Chem. C 2012, 116, 24233−24238

PAPER

To the pore and through and kinetics of helium ir polymorphs†

Cite this: *Phys. Chem. Chem. Phys.*, 2013, **15**, 17366

Piotr Kowalczyk,*[a] Julong He,[b] Meng and Artur P. Terzyk[c]

f_{cc}-C_{10}

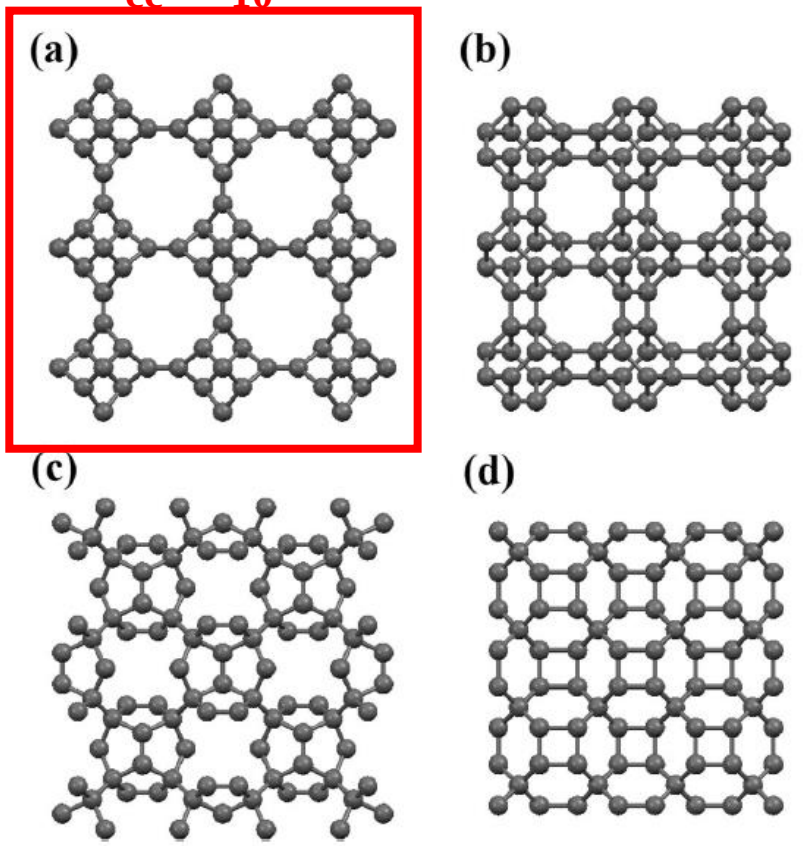

Fig. 1 Crystal structures of the studied cubic carbon polymorphs:[36] (a) fcc-C_{10}, (b) fcc-C_{12}, (c) bcc-C_{20}, and (d) fcc-C_{32}.

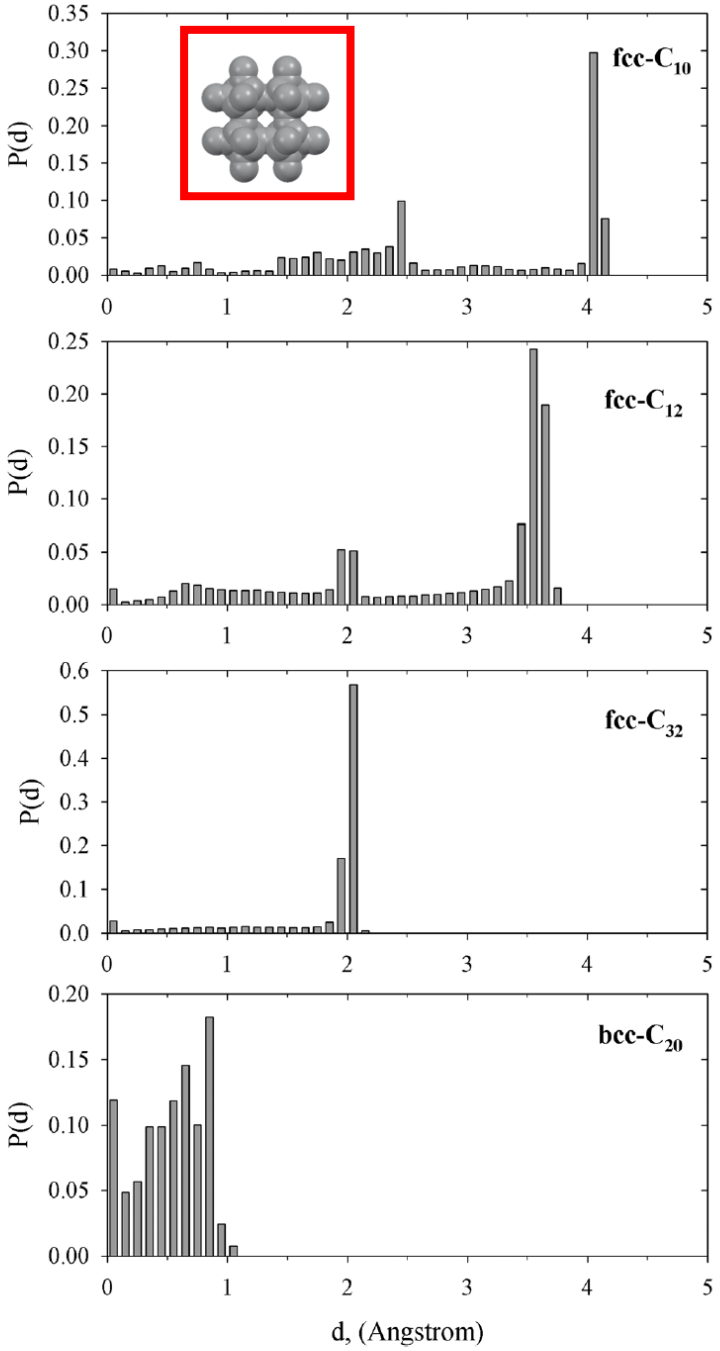

Fig. 3 Pore size distributions of the studied cubic carbon polymorphs computed from the method of Bhattacharya and Gubbins.[37]

298 K

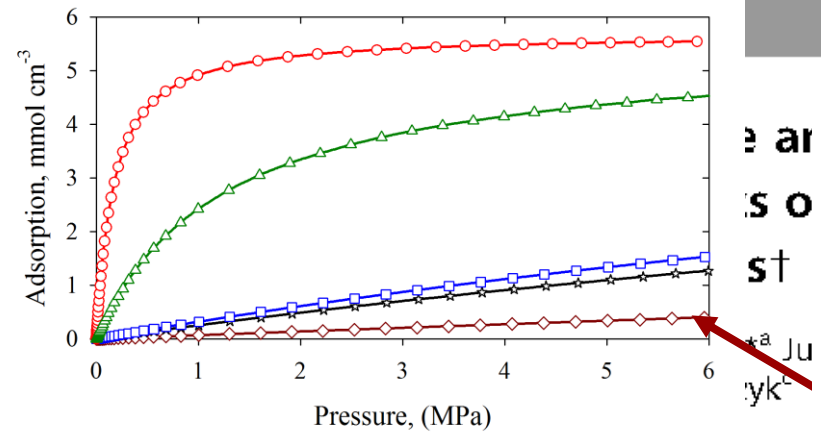

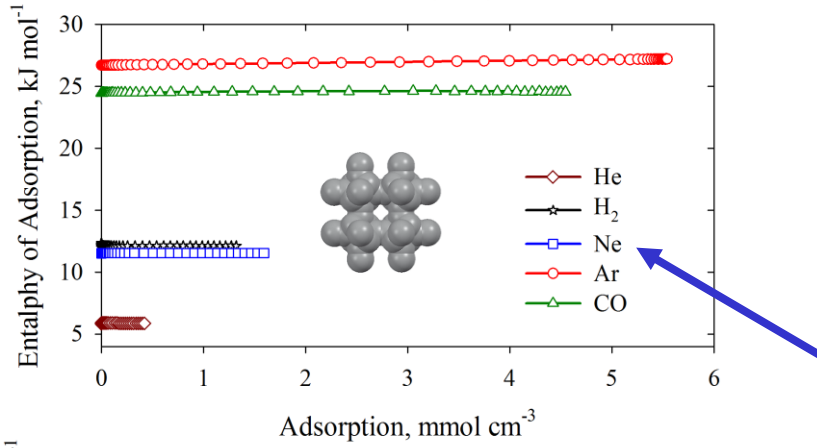

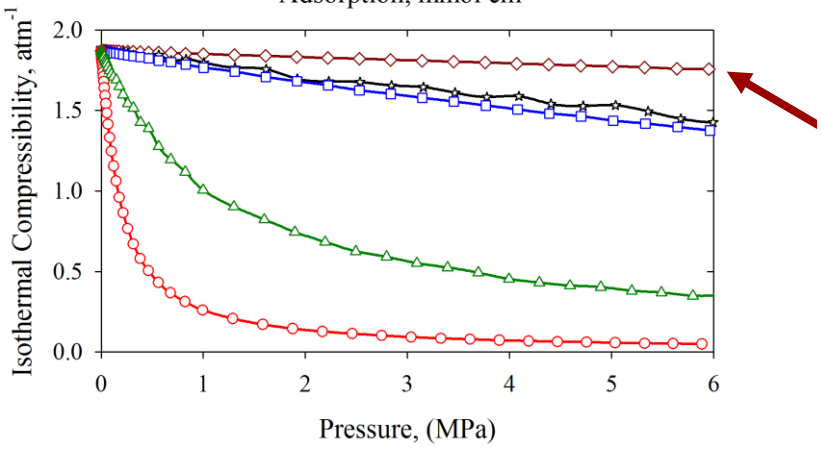

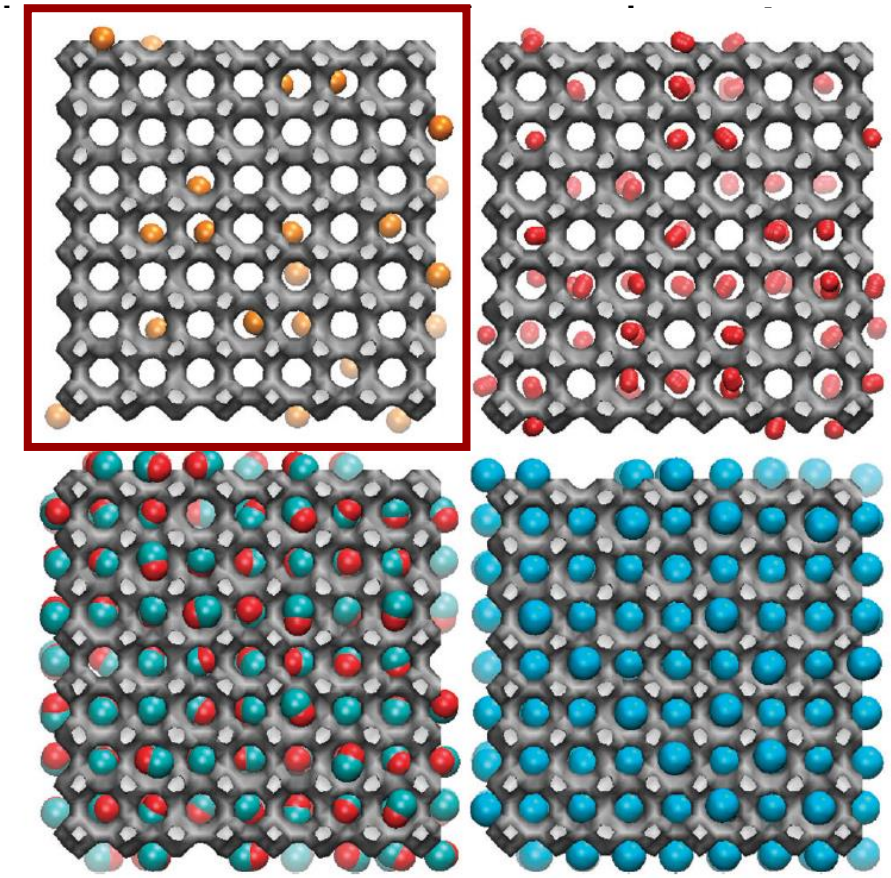

Fig. 5 GCMC snapshot of He, H_2, CO, and Ar adsorbed in the fcc-C_{10} cubic carbon crystal at 6 MPa and 298 K. Under the studied operating conditions, the fcc-C_{10} cubic carbon crystal adsorbs 0.0017 g cm^{-3} of He and 0.22 g cm^{-3} of Ar (volumetric density of liquid He at 4.2 K and liquid Ar at 85.6 K are 0.147 g cm^{-3} and 1.4 g cm^{-3}, respectively).

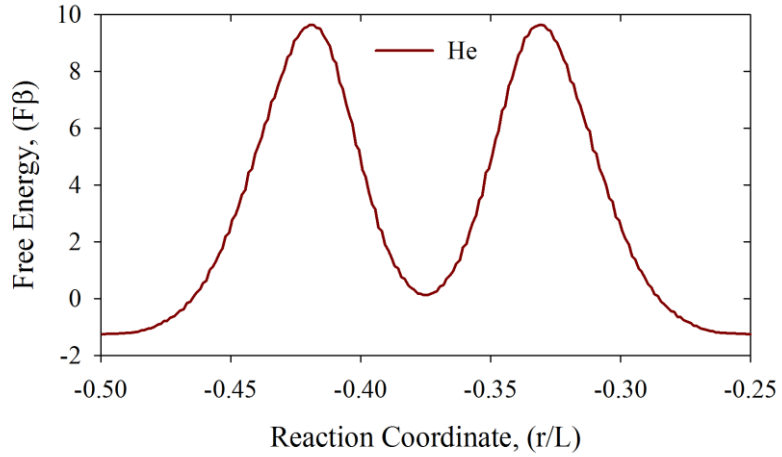
He
Free Energy, (Fβ)
Reaction Coordinate, (r/L)

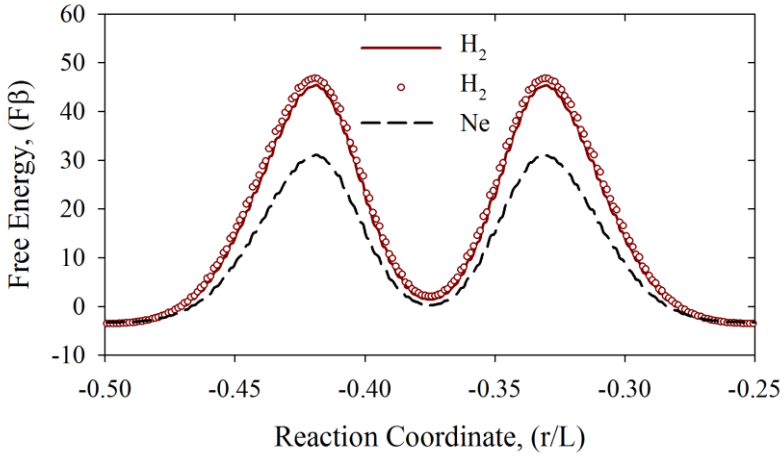
H2
H2
Ne
Free Energy, (Fβ)
Reaction Coordinate, (r/L)

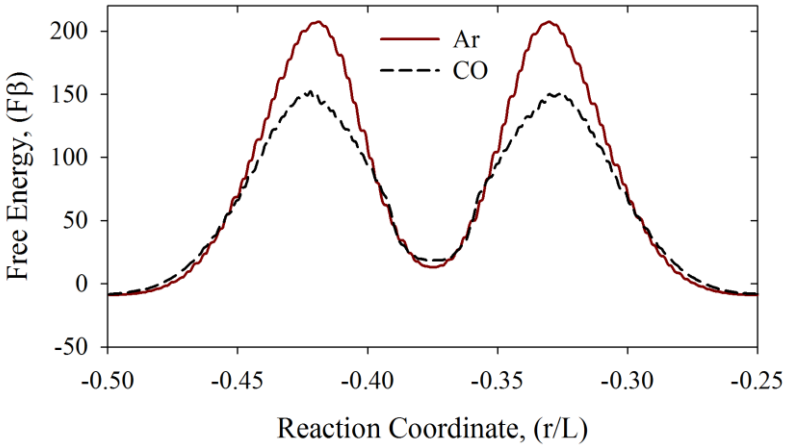
Ar
CO
Free Energy, (Fβ)
Reaction Coordinate, (r/L)

Carbon cavities of fcc-C_{10} carbon polymorph (with effective size of ~3.5-4 Å) are kinetically closed for common gaseous contaminates of helium fluid (including: Ne, Ar, H_2, and CO).

Because the sizes of nanowindows connecting carbon cavities are comparable with the effective size of He atom (~2.556 Å), we predicted a significant resistance for self-diffusion of He in fcc-C_{10} crystal.

Computed self-diffusion coefficients ~ 1.3 10^{-6} – 1.3 10^{-7} cm^2/s for He inside fcc-C_{10} fall in the range characteristic for molecular diffusion in zeolites.

Infrequent "jumps" of He atoms between neighboring carbon cavities and kinetic rejection of other gaseous particles indicate potential application of fcc-C_{10} carbon polymorph for kinetic molecular sieving of He near ambient temperatures.

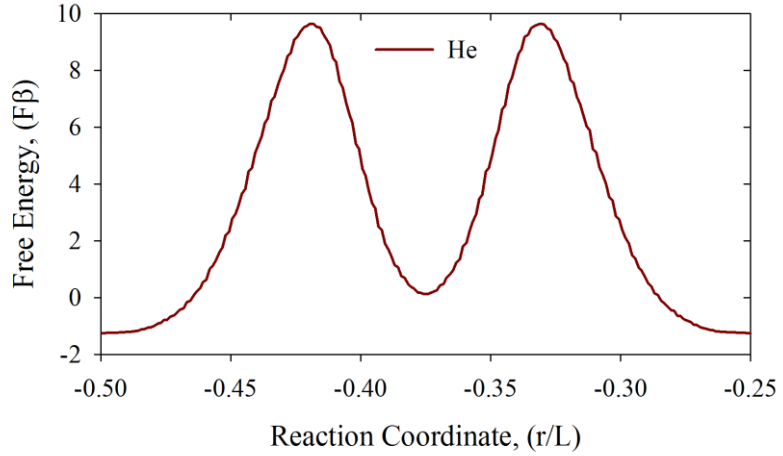

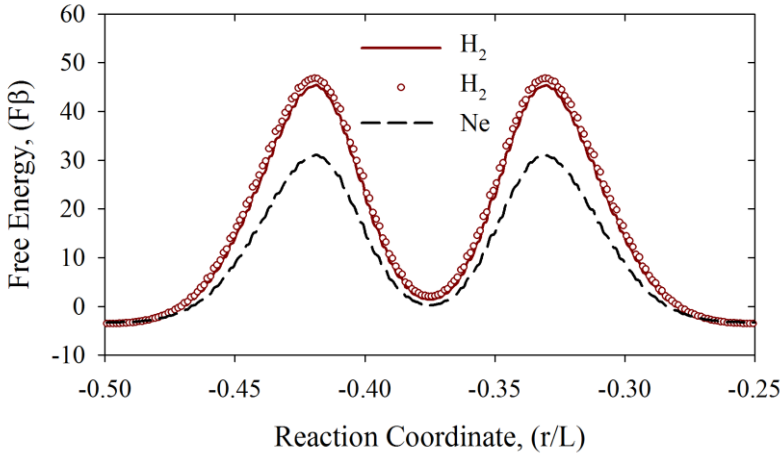

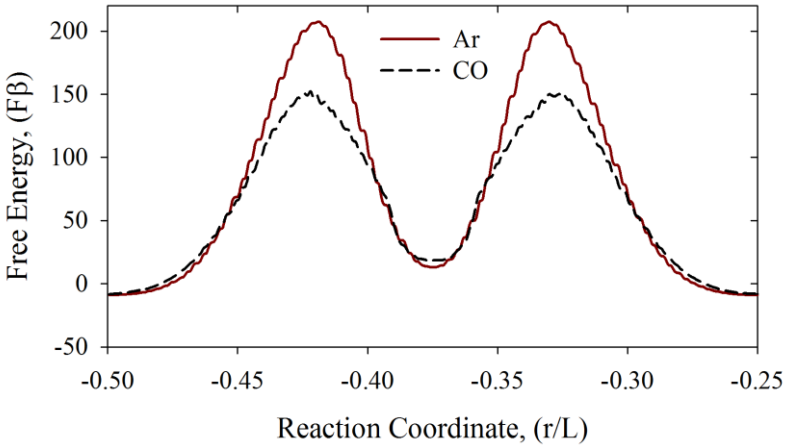

Carbon cavities of fcc-C_{10} carbon polymorph (with effective size of ~3.5-4 Å) are kinetically closed for common gaseous contaminates of helium fluid (including: Ne, Ar, H_2, and CO).

Because the sizes of nanowindows connecting carbon cavities are comparable with the effective size of He atom (~2.556 Å), we predicted a significant resistance for self-diffusion of He in fcc-C_{10} crystal.

Computed self-diffusion coefficients ~ 1.3 10^{-6} – 1.3 10^{-7} cm^2/s for He inside fcc-C_{10} fall in the range characteristic for molecular diffusion in zeolites.

Infrequent "jumps" of He atoms between neighboring carbon cavities and kinetic rejection of other gaseous particles indicate potential application of fcc-C_{10} carbon polymorph for kinetic molecular sieving of He near ambient temperatures.

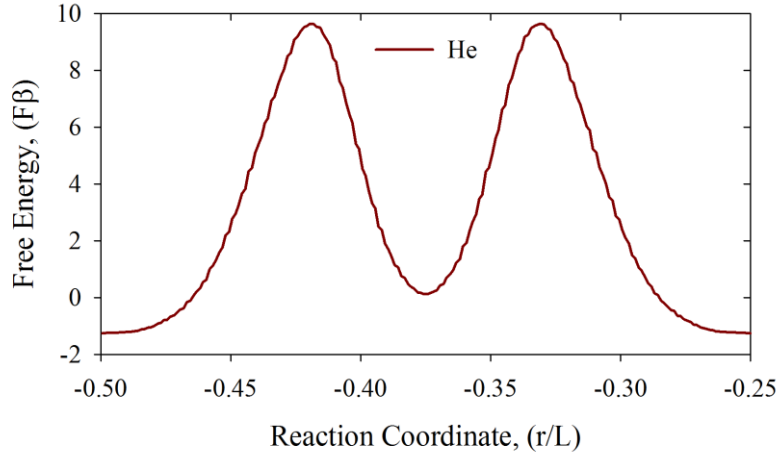

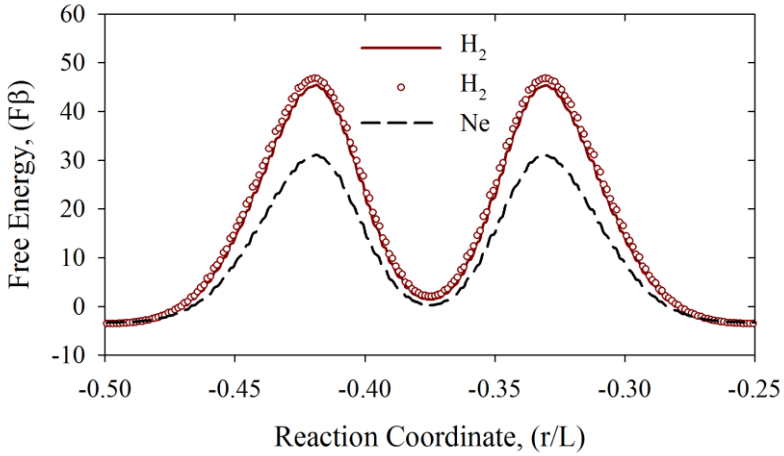

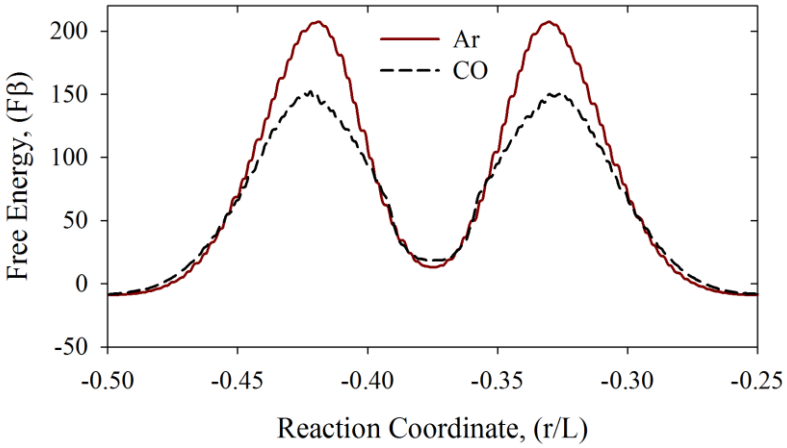

Carbon cavities of fcc-C_{10} carbon polymorph (with effective size of ~3.5-4 Å) are kinetically closed for common gaseous contaminates of helium fluid (including: Ne, Ar, H_2, and CO).

Because the sizes of nanowindows connecting carbon cavities are comparable with the effective size of He atom (~2.556 Å), we predicted a significant resistance for self-diffusion of He in fcc-C_{10} crystal.

Computed self-diffusion coefficients ~ 1.3 10^{-6} – 1.3 10^{-7} cm^2/s for He inside fcc-C_{10} fall in the range characteristic for molecular diffusion in zeolites.

Infrequent "jumps" of He atoms between neighboring carbon cavities and kinetic rejection of other gaseous particles indicate potential application of fcc-C_{10} carbon polymorph for kinetic molecular sieving of He near ambient temperatures.

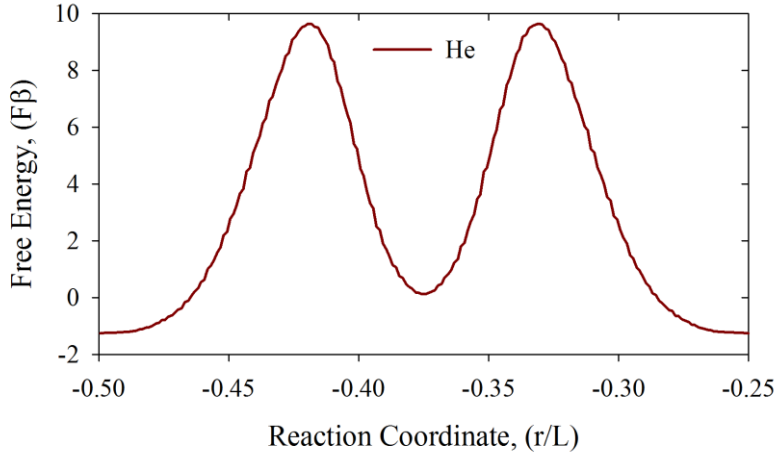

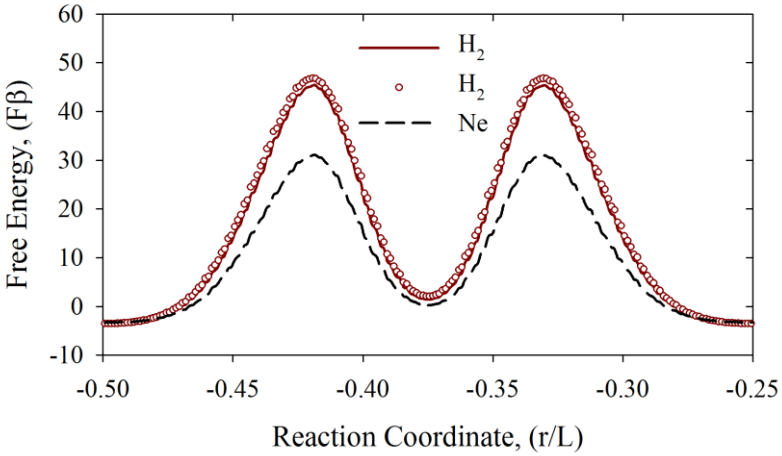

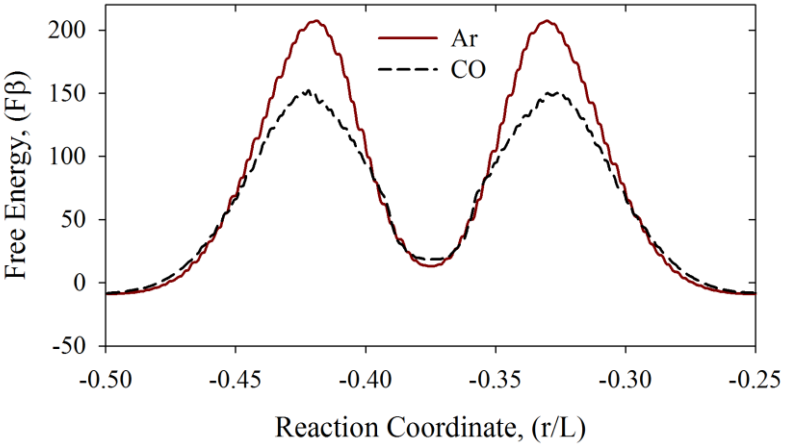

Carbon cavities of fcc-C_{10} carbon polymorph (with effective size of ~3.5-4 Å) are kinetically closed for common gaseous contaminates of helium fluid (including: Ne, Ar, H_2, and CO).

Because the sizes of nanowindows connecting carbon cavities are comparable with the effective size of He atom (~2.556 Å), we predicted a significant resistance for self-diffusion of He in fcc-C_{10} crystal.

Computed self-diffusion coefficients ~ 1.3 10^{-6} – 1.3 10^{-7} cm^2/s for He inside fcc-C_{10} fall in the range characteristic for molecular diffusion in zeolites.

Infrequent "jumps" of He atoms between neighboring carbon cavities and kinetic rejection of other gaseous particles indicate potential application of fcc-C_{10} carbon polymorph for kinetic molecular sieving of He near ambient temperatures.

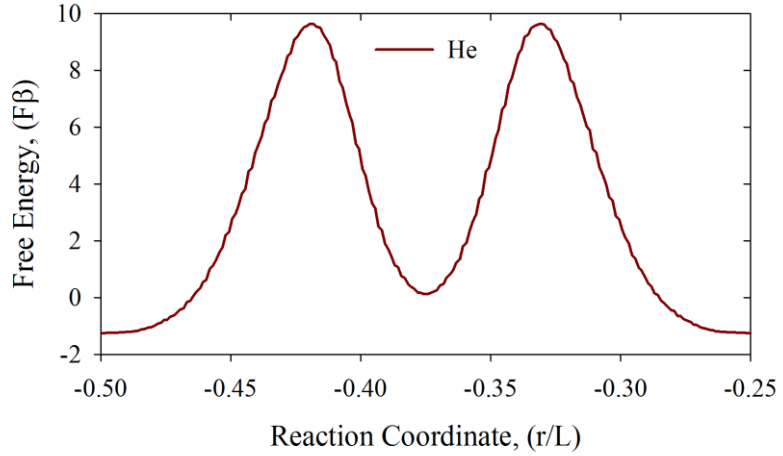

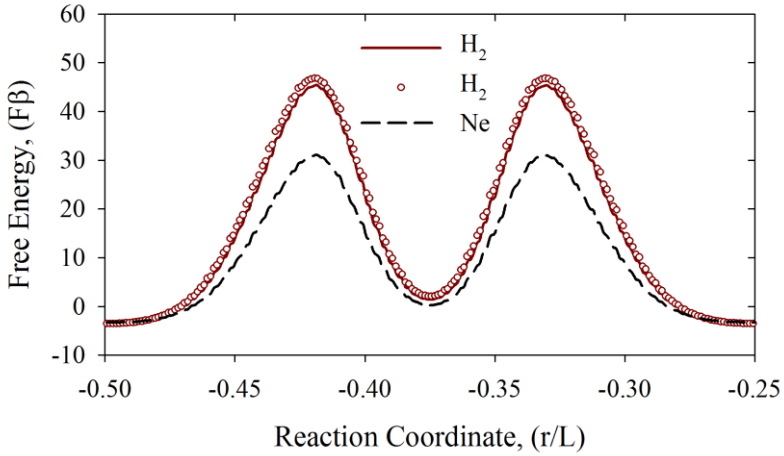

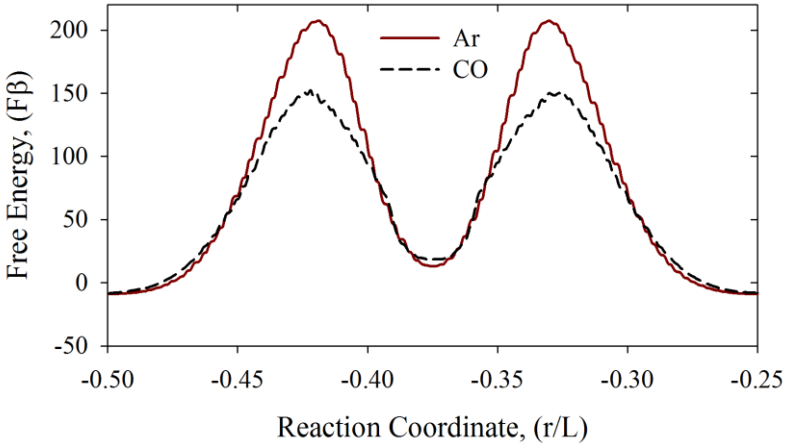

Periodic Table of the Elements

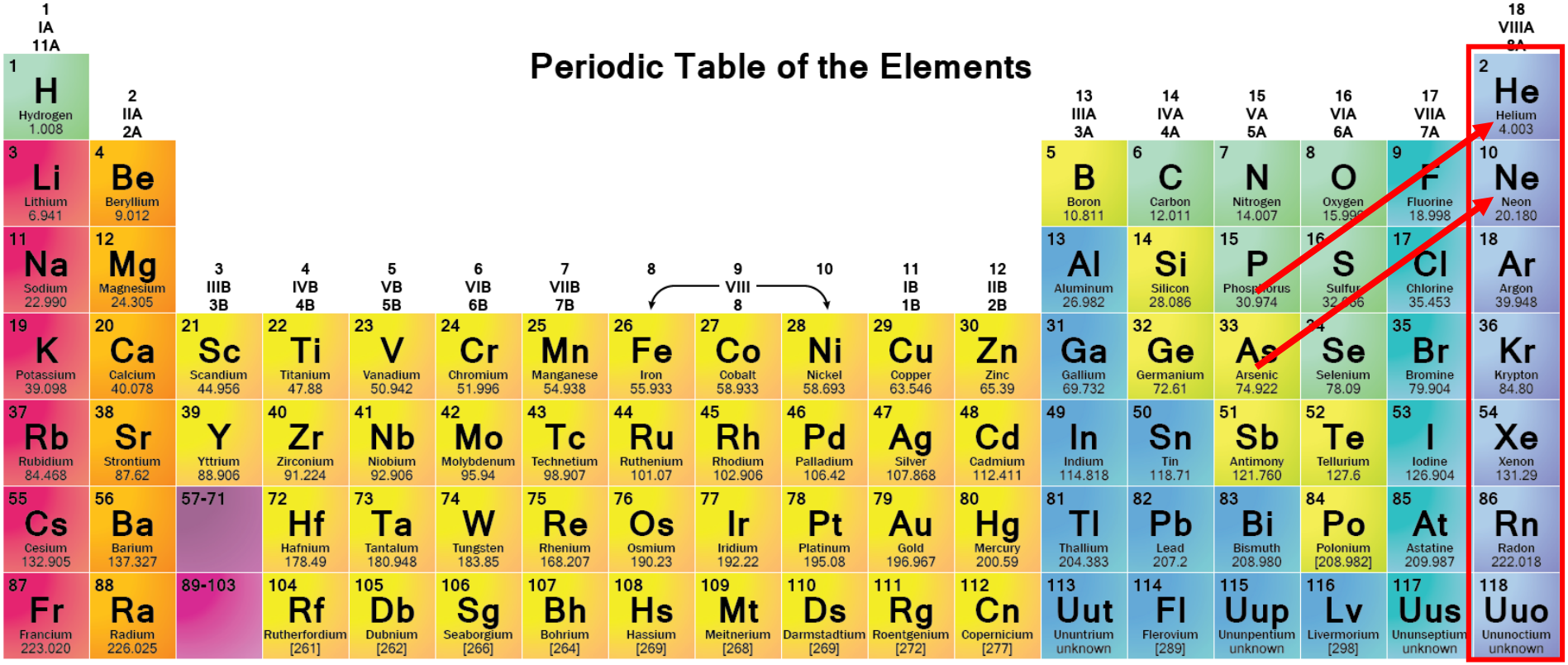

Lanthanide Series	57 La Lanthanum 138.906	58 Ce Cerium 140.115	59 Pr Praseodymium 140.908	60 Nd Neodymium 144.24	61 Pm Promethium 144.913	62 Sm Samarium 150.36	63 Eu Europium 151.966	64 Gd Gadolinium 157.25	65 Tb Terbium 158.925	66 Dy Dysprosium 162.50	67 Ho Holmium 164.930	68 Er Erbium 167.26	69 Tm Thulium 168.934	70 Yb Ytterbium 173.04	71 Lu Lutetium 174.967
Actinide Series	89 Ac Actinium 227.028	90 Th Thorium 232.038	91 Pa Protactinium 231.036	92 U Uranium 238.029	93 Np Neptunium 237.048	94 Pu Plutonium 244.064	95 Am Americium 243.061	96 Cm Curium 247.070	97 Bk Berkelium 247.070	98 Cf Californium 251.080	99 Es Einsteinium [254]	100 Fm Fermium 257.095	101 Md Mendelevium 258.1	102 No Nobelium 259.101	103 Lr Lawrencium [262]

Alkali Metal | Alkaline Earth | Transition Metal | Semimetal | Nonmetal | Basic Metal | Halogen | Noble Gas | Lanthanide | Actinide

OMC

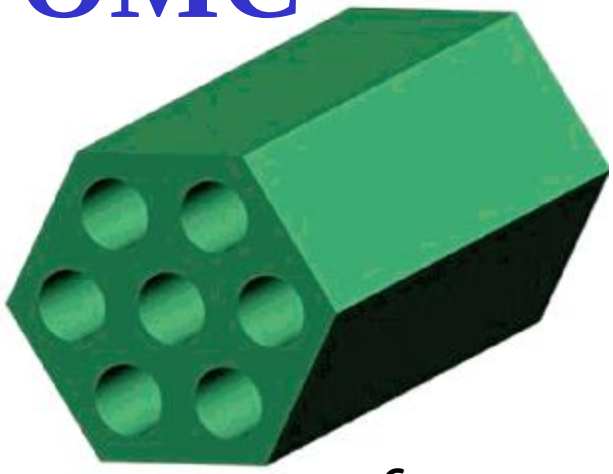

p6mm

SBA-15

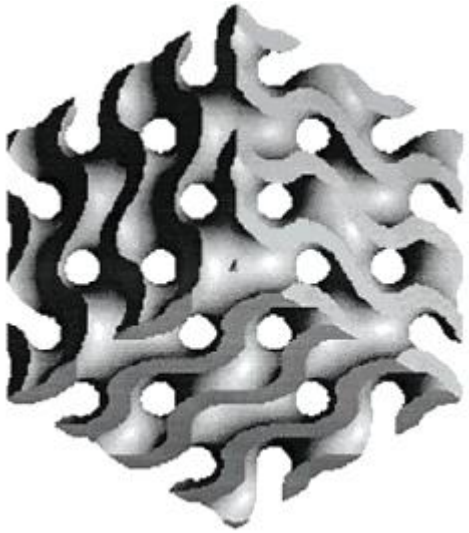

Ia3d,

MCM-48

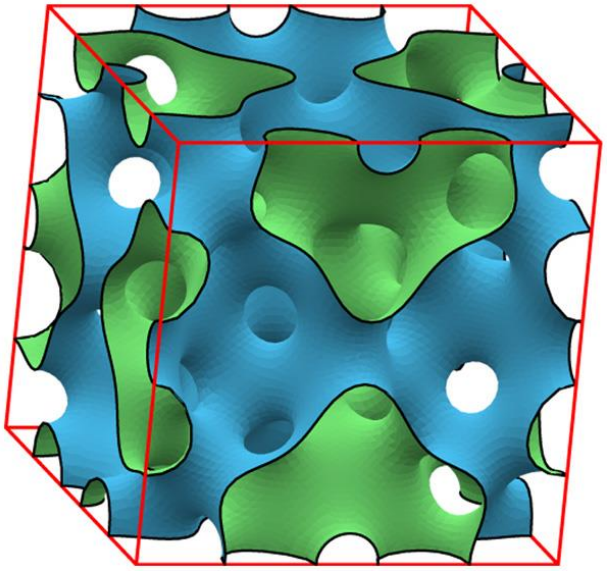

Pm3n

SBA-1 and 6

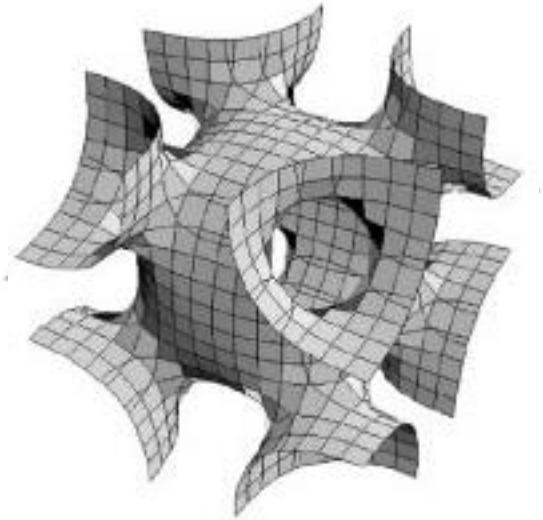

Im3m

SBA-16

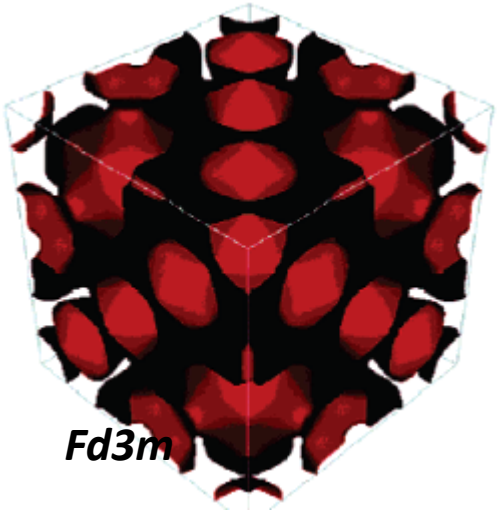

Fd3m

FDU-2

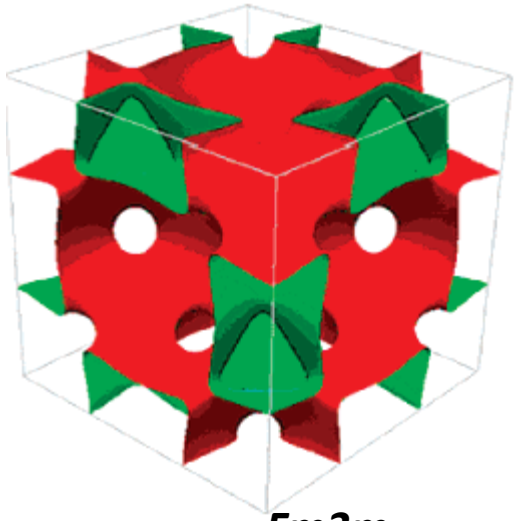

Fm3m.

KIT-5

THE JOURNAL OF PHYSICAL CHEMISTRY C

Article

pubs.acs.org/JPCC

Electrolyte Diffusion in Gyroidal Nanoporous Carbon

Adrien Nicolaï, Joseph Monti, Colin Daniels, and Vincent Meunier*

DOI: 10.1021/jp511919d
J. Phys. Chem. C 2015, 119, 2896−2903

Carbon 96 (2016) 998–1007

Contents lists available at ScienceDirect

Carbon

journal homepage: www.elsevier.com/locate/carbon

Structural, energetic, and electronic properties of gyroidal graphene nanostructures

J.R. Owens [a], C. Daniels [a], A. Nicolaï [a], H. Terrones [a], V. Meunier [a, b, *]

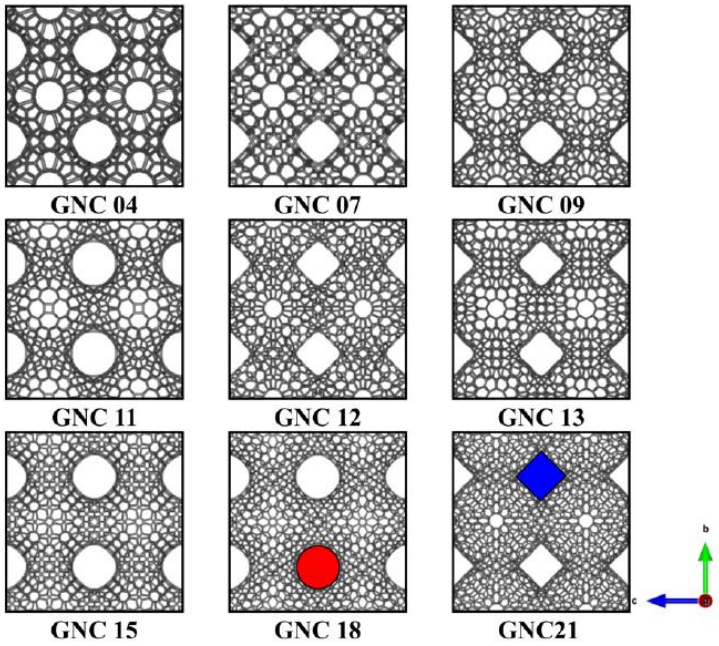

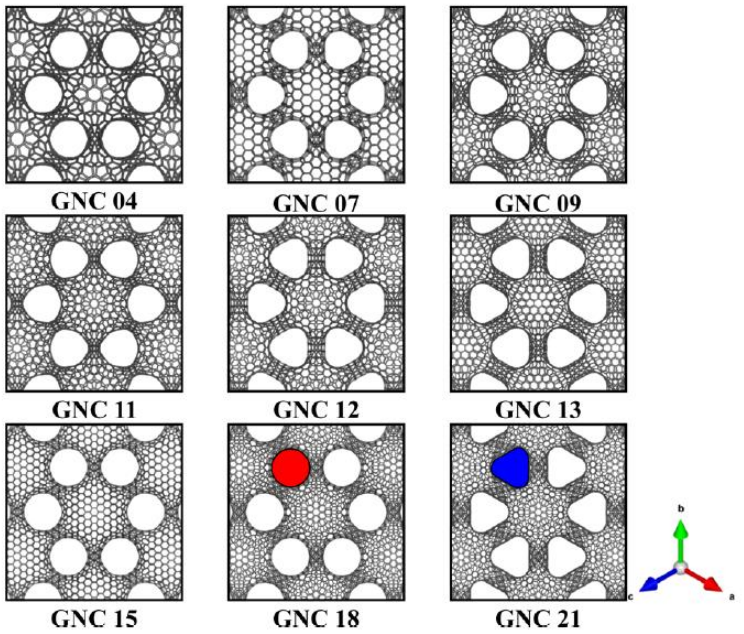

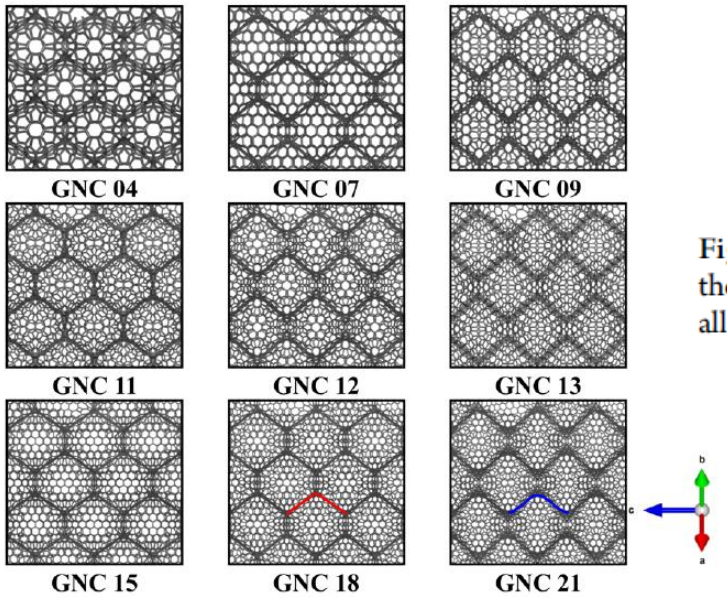

Figure 1. Projection of gyroidal nanoporous carbon structures along the [100] (panel a), [110] (panel b), and [111] direction (panel c) for all gyroids considered in this work.

Type I: G_{16} [001] View

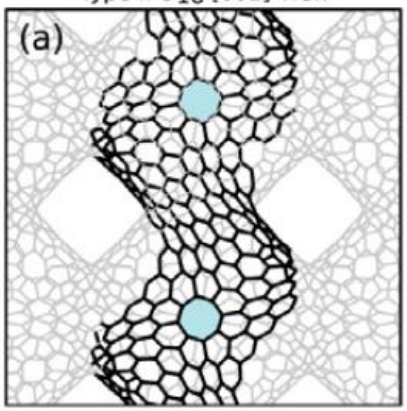

Type II: G_{15} [001] View

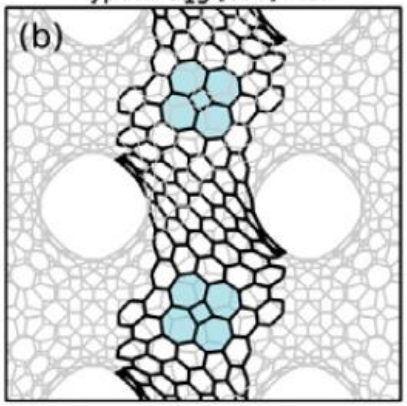

Type III: G_{14} [001] View

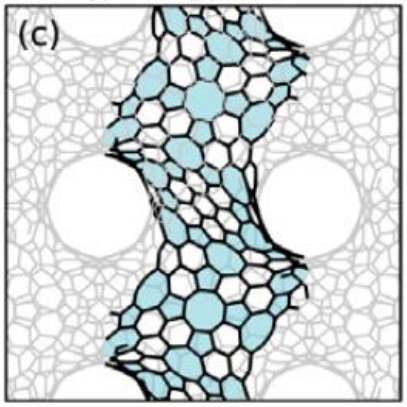

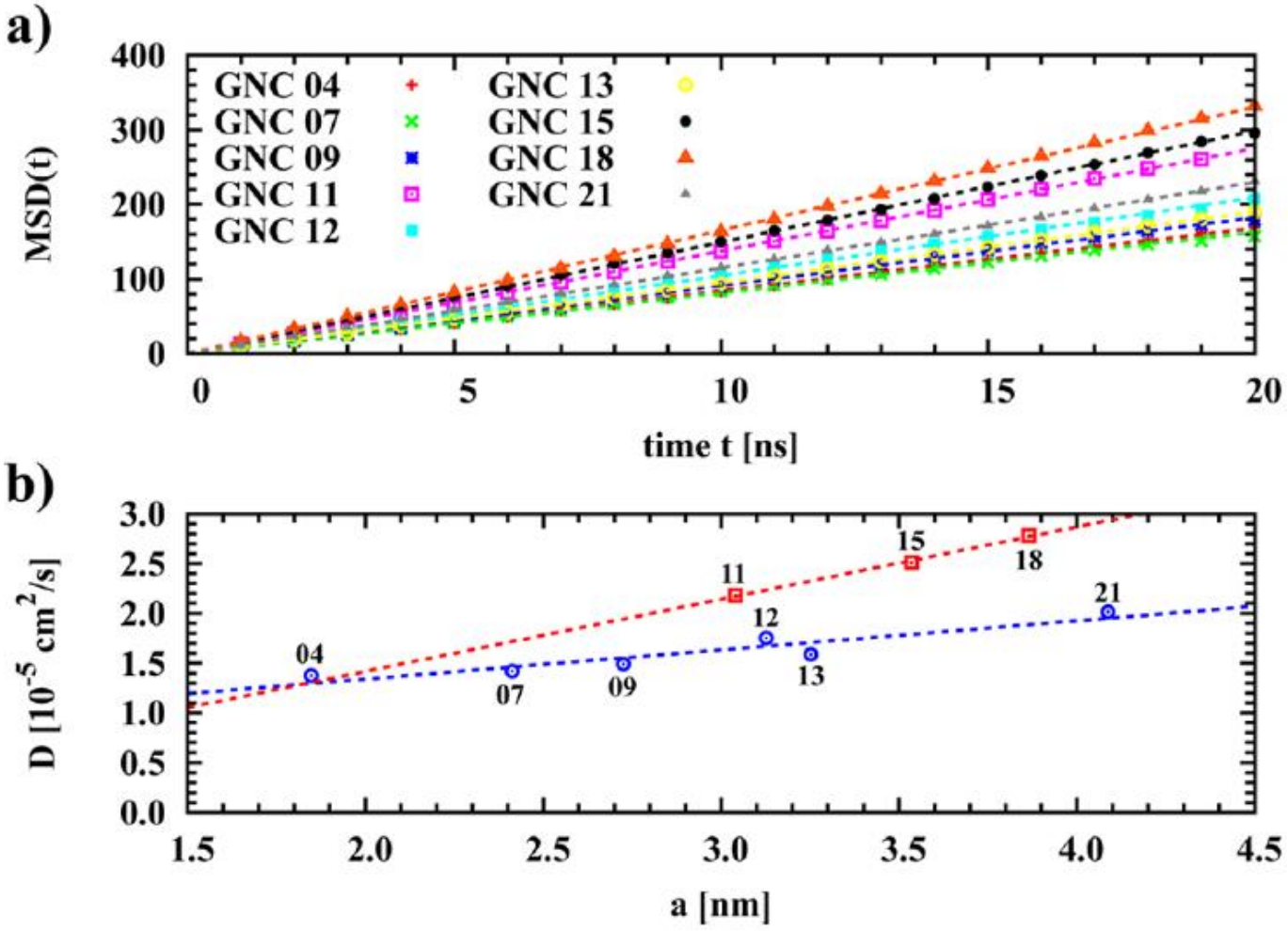

Figure 3. Diffusion properties of water in GNC structures. (a) MSD(t) of water molecules as a function of time computed from MD simulations. Points represent data extracted from MD simulations and lines the best-fit slope. (b) Self-diffusion coefficient D as a function of GNC unit cell parameter a. GNC indices are indicated for clarity. For comparison, the value of bulk TIP3P water using the same MD setup[18] is 5.3×10^{-5} cm^2 s^{-1}.

Condensed Matter Physics, 2016, Vol. 19, No 1, 13003: 1–14
DOI: 10.5488/CMP.19.13003
http://www.icmp.lviv.ua/journal

CONDENSED MATTER PHYSICS

Gyroidal nanoporous carbons — Adsorption and separation properties explored using computer simulations*

S. Furmaniak[1], P.A. Gauden[1], A.P. Terzyk[1], P. Kowalczyk[2]

[1] Faculty of Chemistry, Physicochemistry of Carbon Materials Research Group, Nicolaus Copernicus University in Toruń, Gagarin St. 7, 87–100 Toruń, Poland

[2] School of Engineering and Information Technology, Murdoch University, Murdoch, Western Australia 6150, Australia

CO_2/CH_4, CO_2/N_2, and CH_4/N_2 mixtures

Gyroidal Nanoporous Carbon with Optimally Selective Neon Adsorption and Separation from Helium

Piotr Kowalczyk[*1], Piotr A. Gauden[2], Sylwester Furmaniak[2], Artur P. Terzyk[2], Marek Wiśniewski[2], Jerzy Włoch[3] and Alexander V. Neimark[4]

[1]School of Engineering and Information Technology, Murdoch University, Perth, Western Australia 6150

[2]Faculty of Chemistry, Physicochemistry of Carbon Materials Research Group, Nicolaus Copernicus University in Toruń, Gagarin Street 7, 87-100 Toruń, Poland

[3]Faculty of Chemistry, Synthesis and Modification of Carbon Materials Research Group, Nicolaus Copernicus University in Toruń, Gagarin Street 7, 87-100 Toruń , Poland

[4]Department of Chemical and Biochemical Engineering, Rutgers, The State University of New Jersey, 98 Brett Road, Piscataway, New Jersey 08854-8058, United States

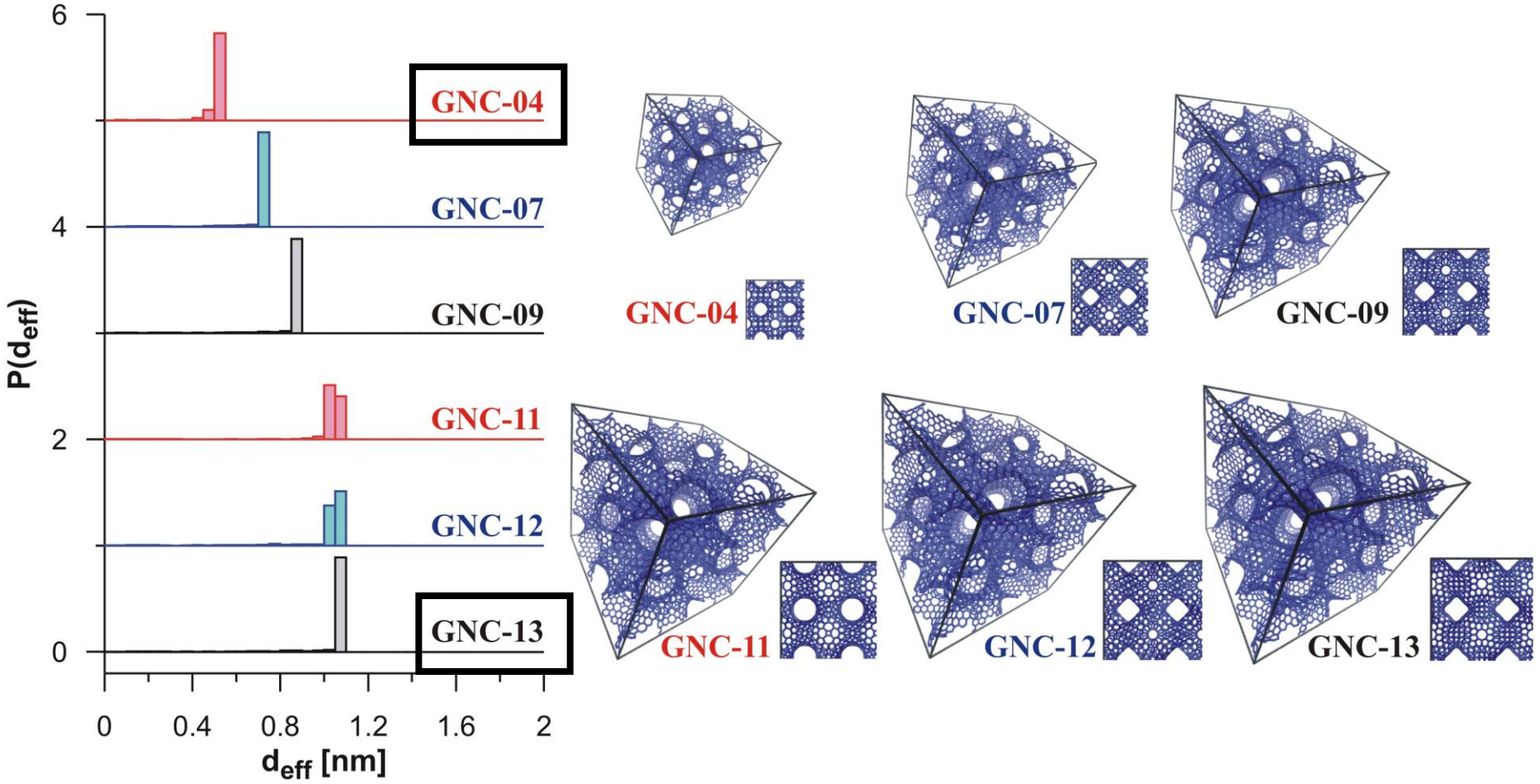
6
4
2
0
P(d_eff)
GNC-04
GNC-07
GNC-09
GNC-11
GNC-12
GNC-13
0
0.4
0.8
1.2
1.6
2
d_eff [nm]
GNC-04
GNC-07
GNC-09
GNC-11
GNC-12
GNC-13

77 K

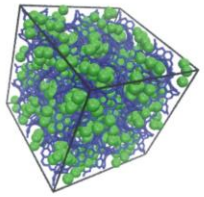

Ne: GNC-04

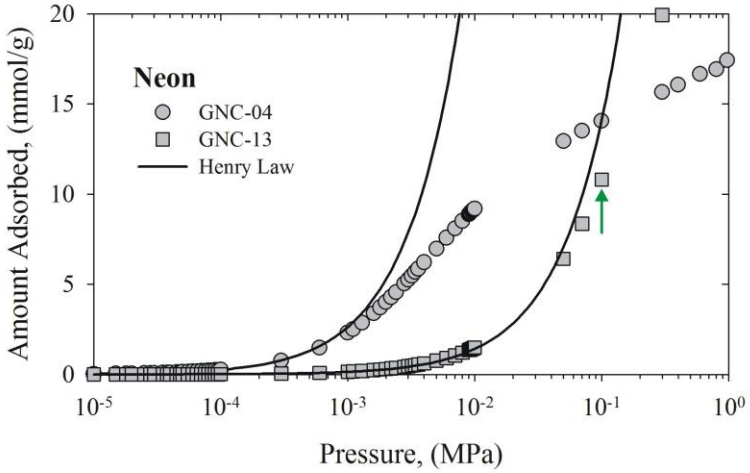

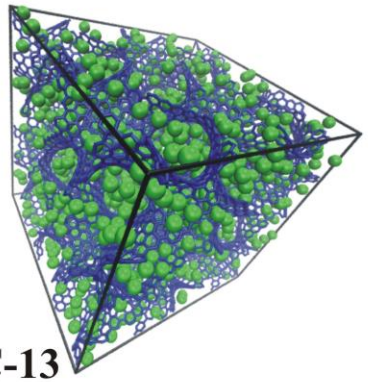

Ne: GNC-13

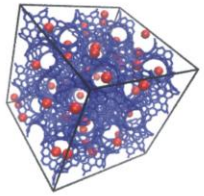

He: GNC-04

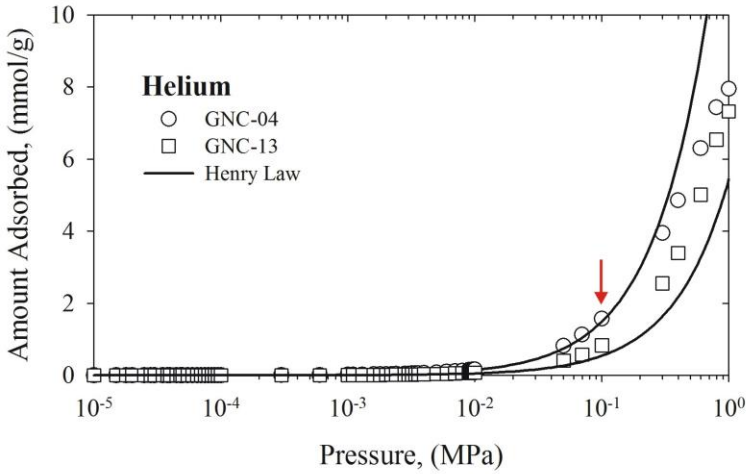

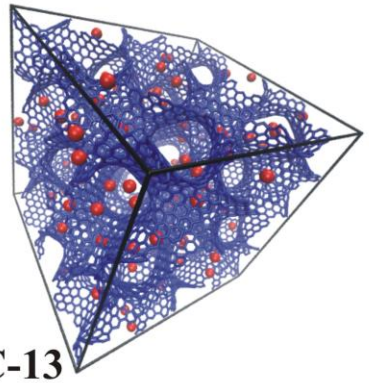

He: GNC-13

He
GNC-04
T = 77 K
p = 0.01 MPa

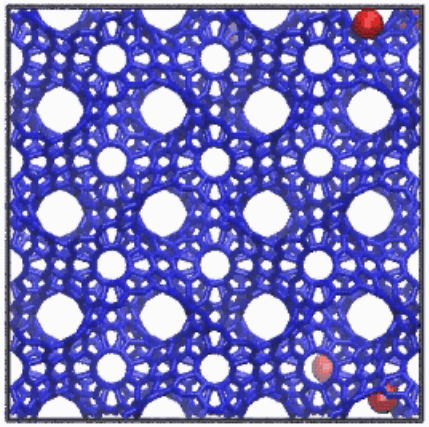

Ne
GNC-04
T = 77 K
p = 0.01 MPa

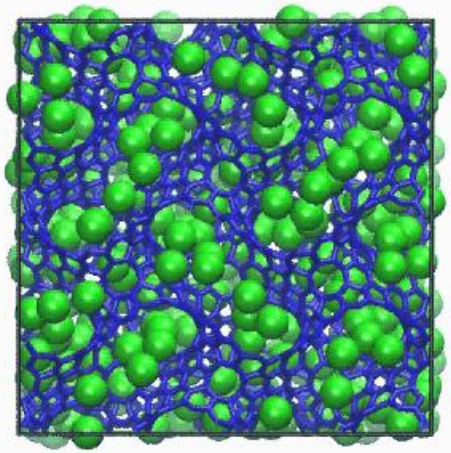

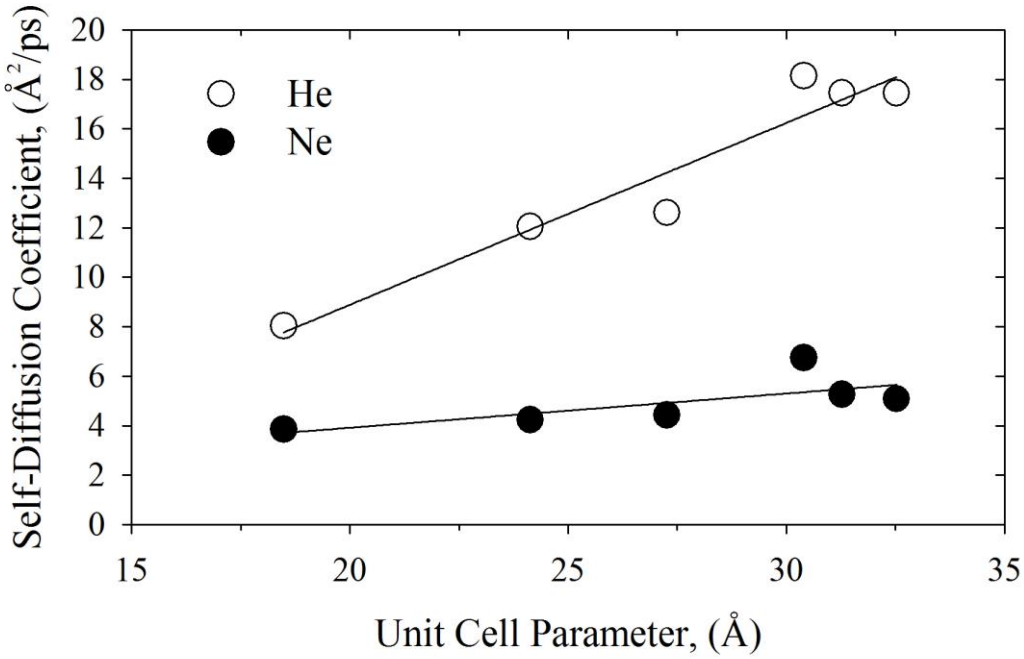
Self-Diffusion Coefficient, (Å²/ps)
He
Ne
Unit Cell Parameter, (Å)

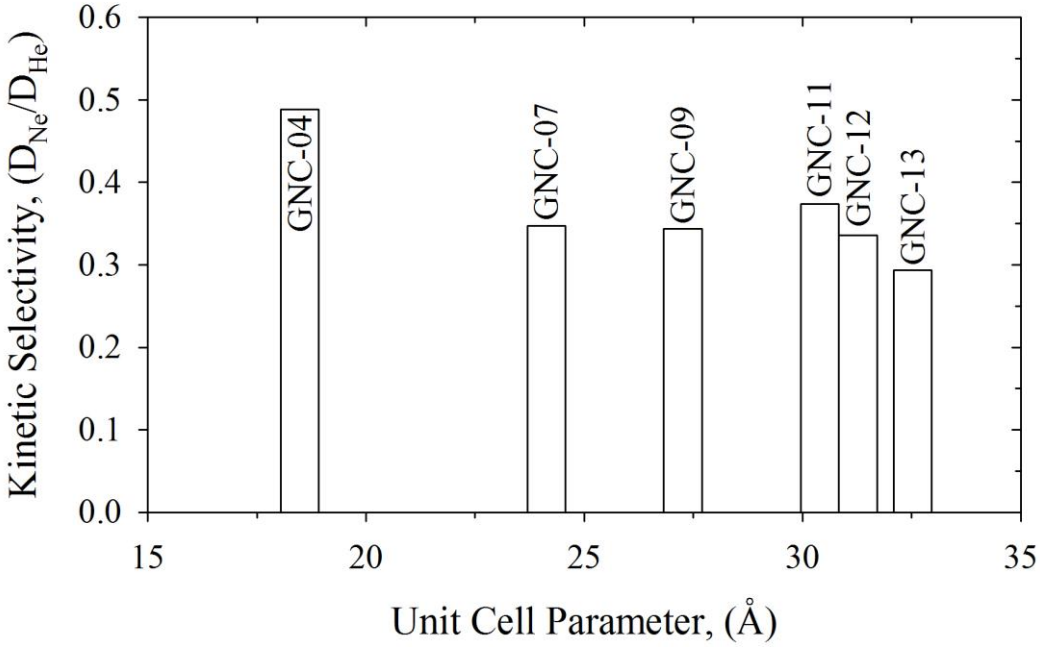
Kinetic Selectivity, (D_Ne/D_He)
GNC-04
GNC-07
GNC-09
GNC-11
GNC-12
GNC-13
Unit Cell Parameter, (Å)

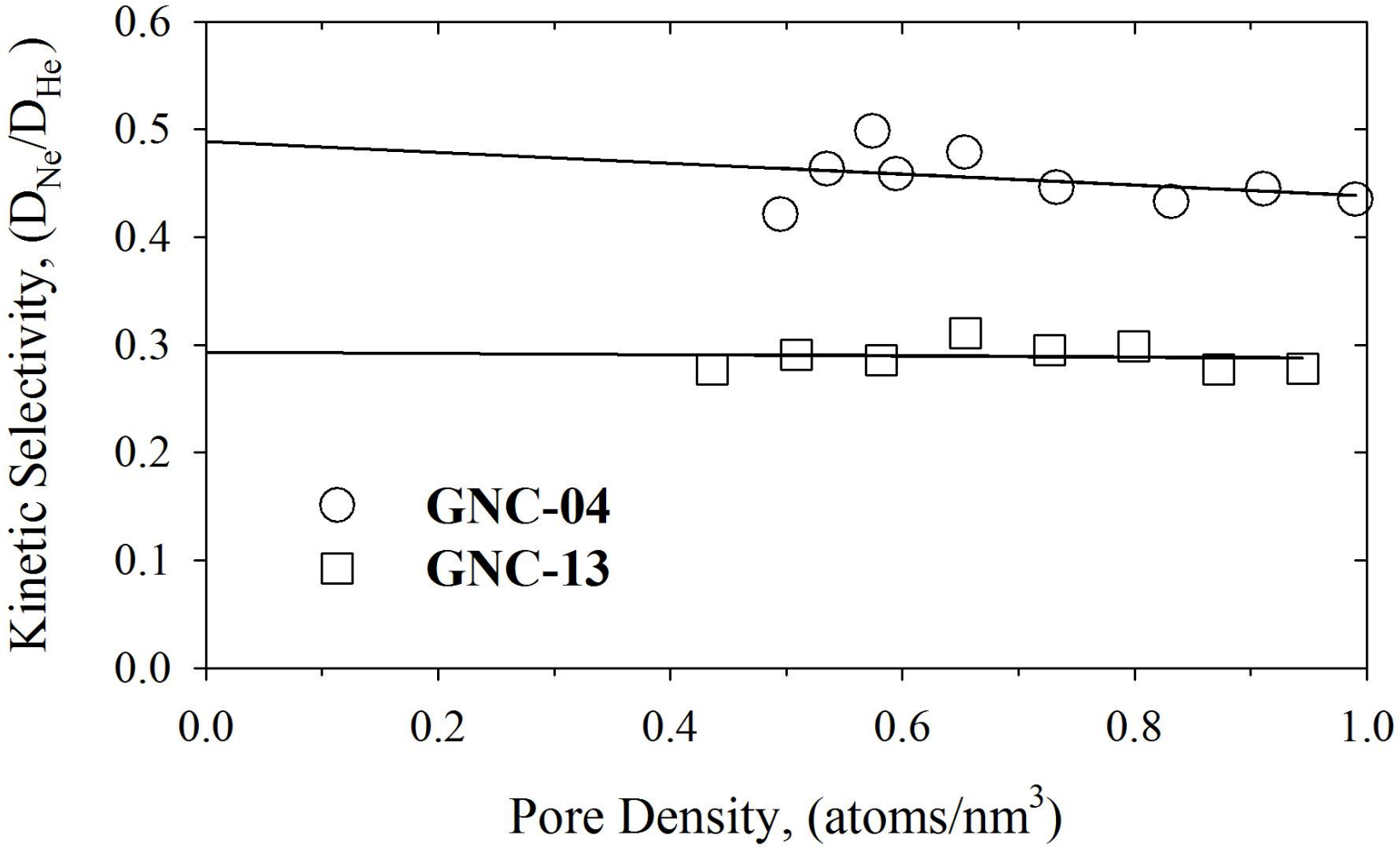
Kinetic Selectivity, (D_{Ne}/D_{He})
0.6
0.5
0.4
0.3
0.2
0.1
0.0
0.0
0.2
0.4
0.6
0.8
1.0
Pore Density, (atoms/nm^3)
GNC-04
GNC-13

We find that selective separation of Ne from diluted Ne-He mixtures on microporous GNCs is driven by **preferential adsorption of Ne at 77 K.**

High adsorption-driven selectivity of Ne over He at zero coverage is compensated by an unfavourable Ne/He kinetic selectivity (e.g. faster diffusion of He).

A detailed analysis of theoretical and simulation results indicates that precise tuning of curved graphene ultramicropores in gyroidal carbon networks to ~0.53 nm is a key for fabrication of selective carbon membranes for cryogenic separation technologies.

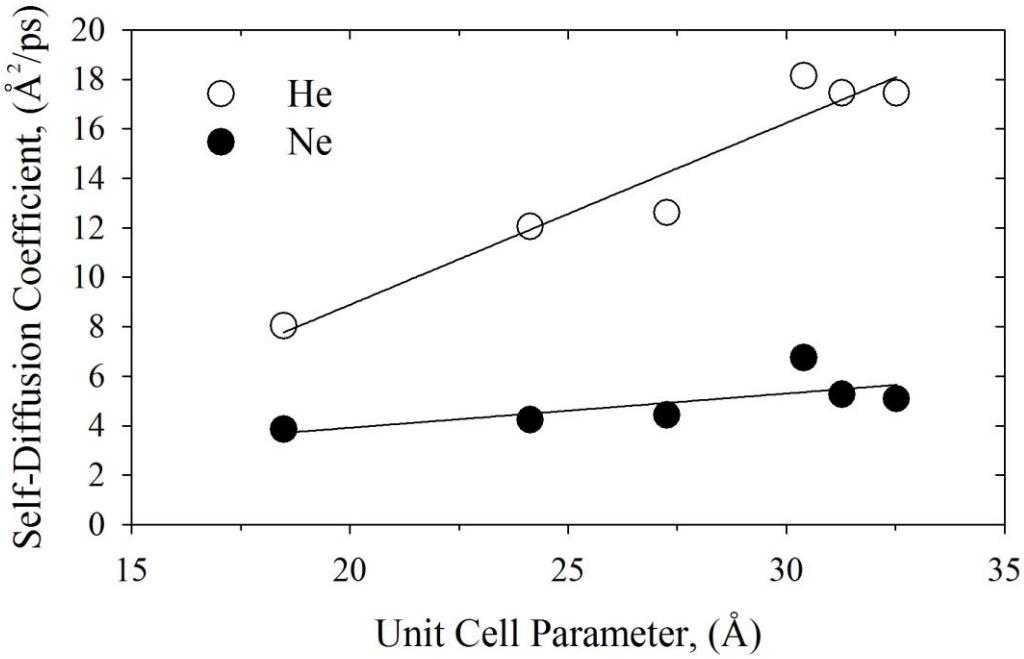

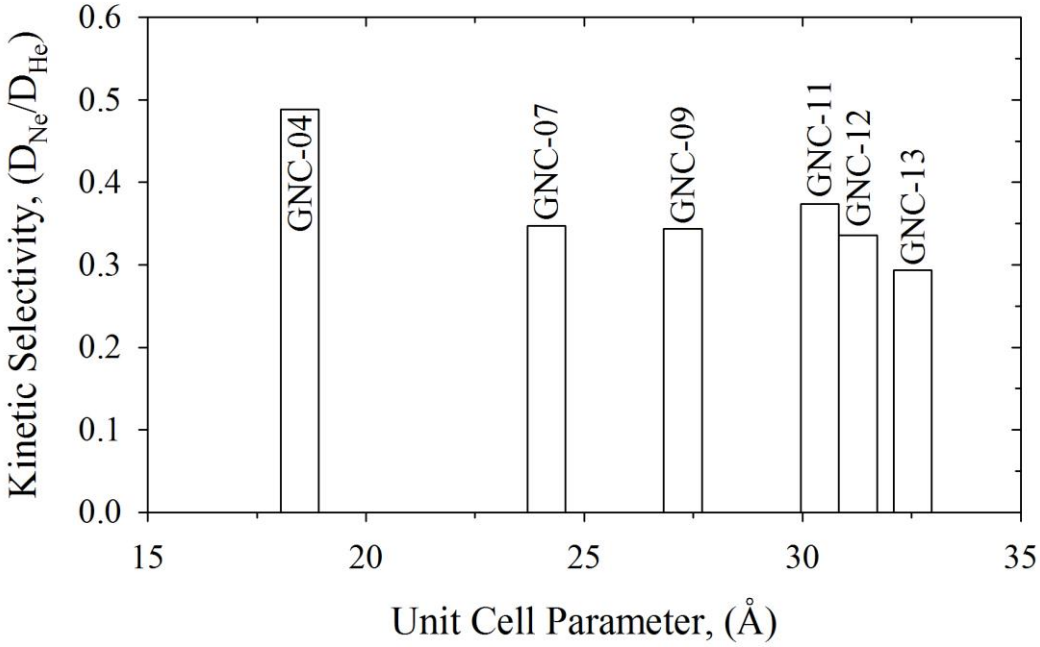

We find that selective separation of Ne from diluted Ne-He mixtures on microporous GNCs is driven by preferential adsorption of Ne at 77 K.

High adsorption-driven selectivity of Ne over He at zero coverage **is compensated** by an unfavourable Ne/He kinetic selectivity (e.g. **faster diffusion of He**).

A detailed analysis of theoretical and simulation results indicates that precise tuning of curved graphene ultramicropores in gyroidal carbon networks to ~0.53 nm is a key for fabrication of selective carbon membranes for cryogenic separation technologies.

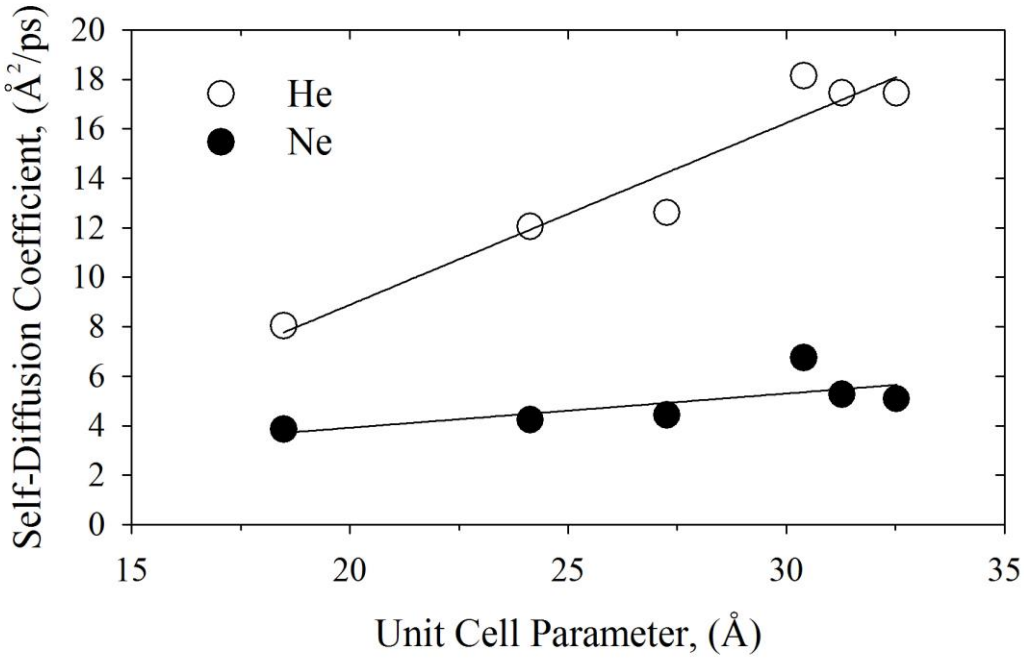

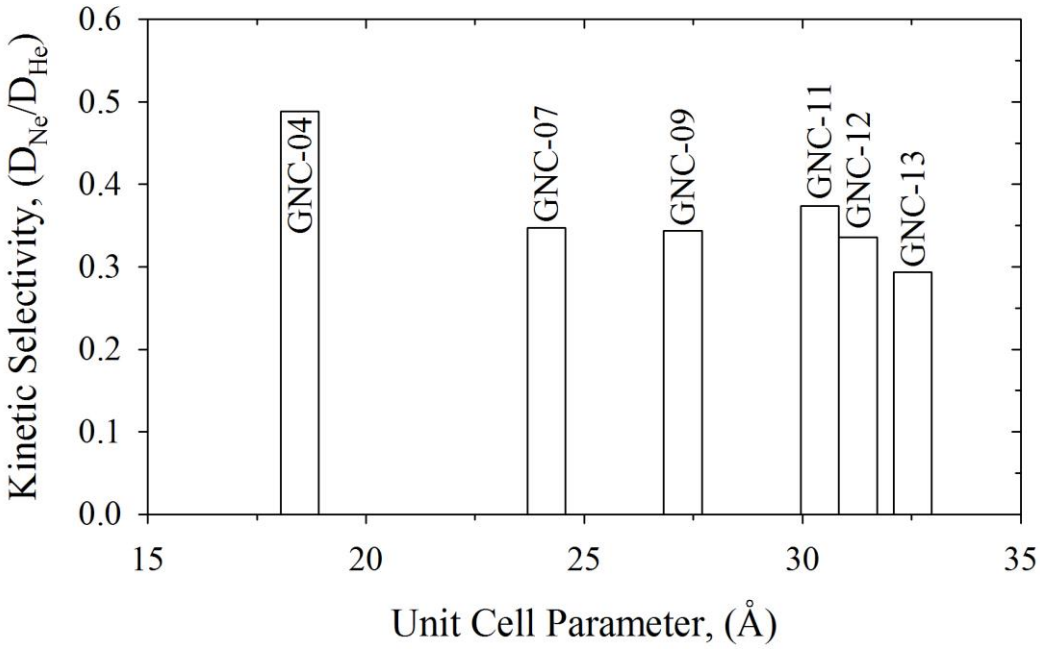

We find that selective separation of Ne from diluted Ne-He mixtures on microporous GNCs is driven by preferential adsorption of Ne at 77 K.

High adsorption-driven selectivity of Ne over He at zero coverage is compensated by an unfavourable Ne/He kinetic selectivity (e.g. faster diffusion of He).

A detailed analysis of theoretical and simulation results indicates that precise tuning of curved graphene ultramicropores in **gyroidal carbon networks to ~0.53 nm is a key for fabrication of selective carbon membranes for cryogenic separation technologies.**

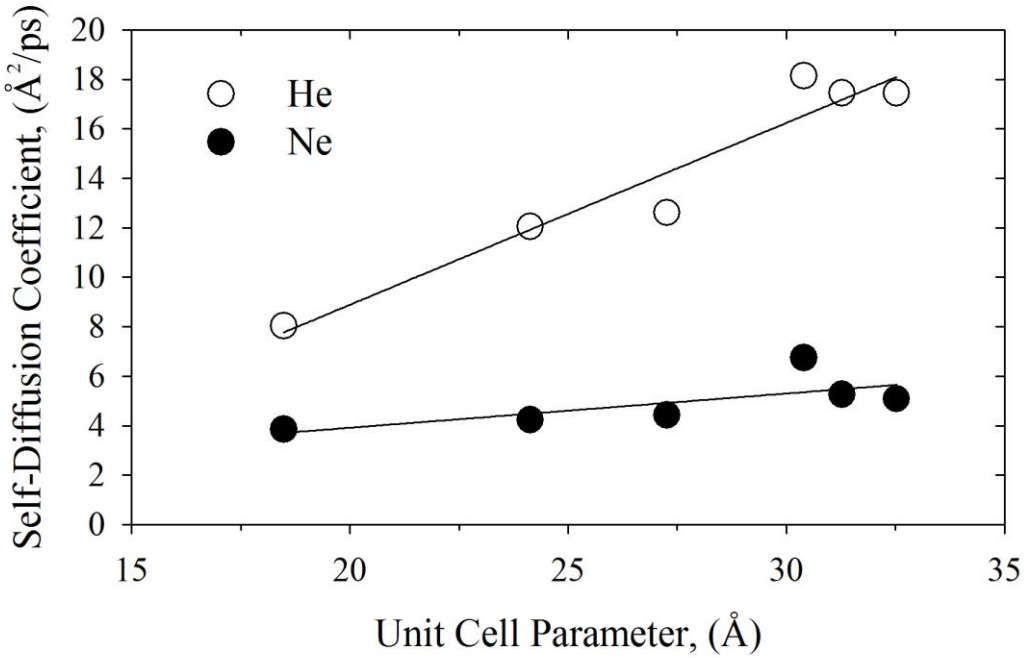

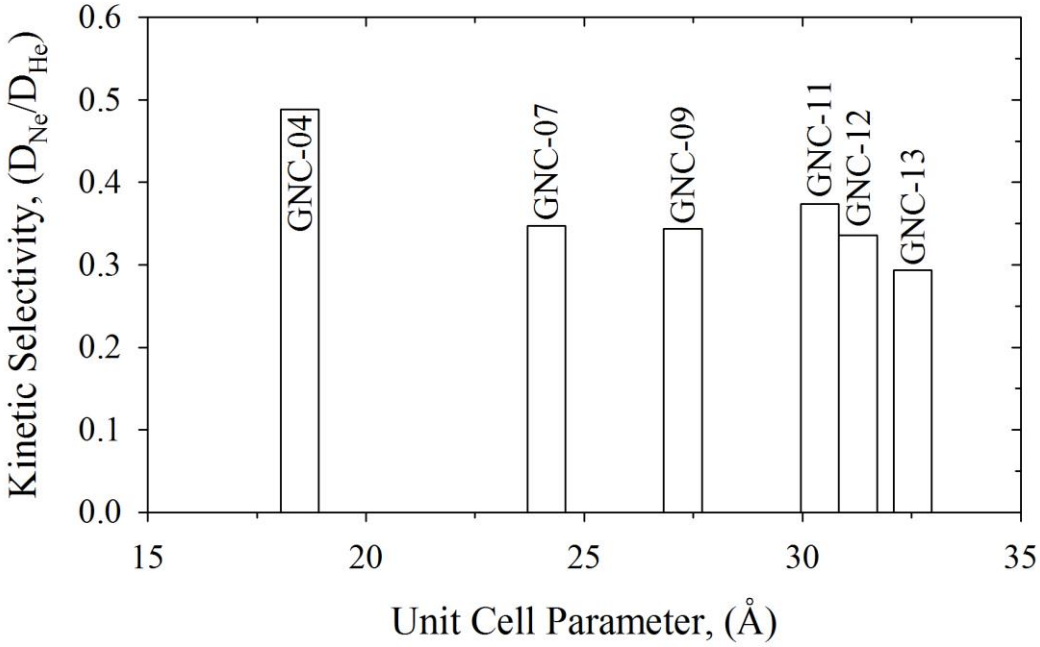

SCIENCE ADVANCES | RESEARCH ARTICLE

MATERIALS SCIENCE

The mechanics and design of a lightweight three-dimensional graphene assembly

Zhao Qin,[1]* Gang Seob Jung,[1]* Min Jeong Kang,[1] Markus J. Buehler[1,2]†

a high-resolution and multimaterial 3D printer, Object500, made by Stratasys, which allowed us to print complex geometries at 20-mm resolution

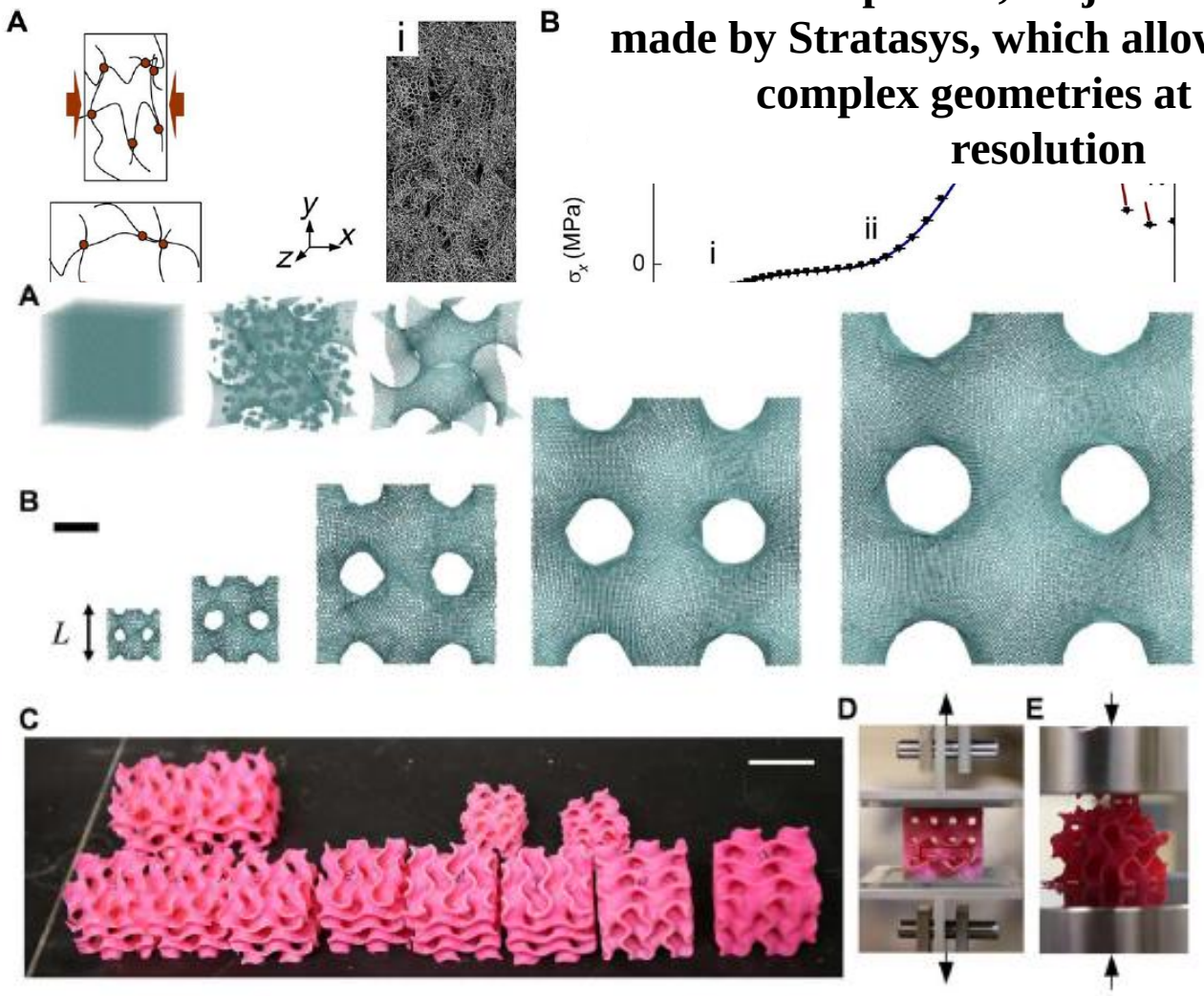

Fig. 4. Different atomistic and 3D-printed models of gyroid geometry for mechanical tests. (**A**) Simulation snapshots taken during the modeling of the atomic 3D graphene structure with gyroid geometry, representing key procedures including (i) generating the coordinate of uniformly distributed carbon atoms based on the fcc structure, (ii) generating a gyroid structure with a triangular lattice feature, and (iii) refinement of the modified geometry from a gyroid with a triangular lattice to one with a hexagonal lattice. (**B**) Five models of gyroid graphene with different length constants of $L = 3, 5, 10, 15$, and 20 nm from left to right. Scale bar, 25 nm. (**C**) 3D printed samples of the gyroid structure of various L values and wall thicknesses. Scale bar, 25 cm. The tensile and compressive tests on the 3D printed sample are shown in (**D**) and (**E**), respectively.

Periodic Table of the Elements

1 IA 11A	2 IIA 2A	3 IIIB 3B	4 IVB 4B	5 VB 5B	6 VIB 6B	7 VIIB 7B	8	9 VIII 8	10	11 IB 1B	12 IIB 2B	13 IIIA 3A	14 IVA 4A	15 VA 5A	16 VIA 6A	17 VIIA 7A	18 VIIIA 8A
1 H Hydrogen 1.008																	2 He Helium 4.003
3 Li Lithium 6.941	4 Be Beryllium 9.012											5 B Boron 10.811	6 C Carbon 12.011	7 N Nitrogen 14.007	8 O Oxygen 15.999	9 F Fluorine 18.998	10 Ne Neon 20.180
11 Na Sodium 22.990	12 Mg Magnesium 24.305											13 Al Aluminum 26.982	14 Si Silicon 28.086	15 P Phosphorus 30.974	16 S Sulfur 32.066	17 Cl Chlorine 35.453	18 Ar Argon 39.948
19 K Potassium 39.098	20 Ca Calcium 40.078	21 Sc Scandium 44.956	22 Ti Titanium 47.88	23 V Vanadium 50.942	24 Cr Chromium 51.996	25 Mn Manganese 54.938	26 Fe Iron 55.933	27 Co Cobalt 58.933	28 Ni Nickel 58.693	29 Cu Copper 63.546	30 Zn Zinc 65.39	31 Ga Gallium 69.732	32 Ge Germanium 72.61	33 As Arsenic 74.922	34 Se Selenium 78.09	35 Br Bromine 79.904	36 Kr Krypton 84.80
37 Rb Rubidium 84.468	38 Sr Strontium 87.62	39 Y Yttrium 88.906	40 Zr Zirconium 91.224	41 Nb Niobium 92.906	42 Mo Molybdenum 95.94	43 Tc Technetium 98.907	44 Ru Ruthenium 101.07	45 Rh Rhodium 102.906	46 Pd Palladium 106.42	47 Ag Silver 107.868	48 Cd Cadmium 112.411	49 In Indium 114.818	50 Sn Tin 118.71	51 Sb Antimony 121.760	52 Te Tellurium 127.6	53 I Iodine 126.904	54 Xe Xenon 131.29
55 Cs Cesium 132.905	56 Ba Barium 137.327	57-71	72 Hf Hafnium 178.49	73 Ta Tantalum 180.948	74 W Tungsten 183.85	75 Re Rhenium 168.207	76 Os Osmium 190.23	77 Ir Iridium 192.22	78 Pt Platinum 195.08	79 Au Gold 196.967	80 Hg Mercury 200.59	81 Tl Thallium 204.383	82 Pb Lead 207.2	83 Bi Bismuth 208.980	84 Po Polonium [208.982]	85 At Astatine 209.987	86 Rn Radon 222.018
87 Fr Francium 223.020	88 Ra Radium 226.025	89-103	104 Rf Rutherfordium [261]	105 Db Dubnium [262]	106 Sg Seaborgium [266]	107 Bh Bohrium [264]	108 Hs Hassium [269]	109 Mt Meitnerium [268]	110 Ds Darmstadtium [269]	111 Rg Roentgenium [272]	112 Cn Copernicium [277]	113 Uut Ununtrium unknown	114 Fl Flerovium [289]	115 Uup Ununpentium unknown	116 Lv Livermorium [298]	117 Uus Ununseptium unknown	118 Uuo Ununoctium unknown

Lanthanide Series	57 La Lanthanum 138.906	58 Ce Cerium 140.115	59 Pr Praseodymium 140.908	60 Nd Neodymium 144.24	61 Pm Promethium 144.913	62 Sm Samarium 150.36	63 Eu Europium 151.966	64 Gd Gadolinium 157.25	65 Tb Terbium 158.925	66 Dy Dysprosium 162.50	67 Ho Holmium 164.930	68 Er Erbium 167.26	69 Tm Thulium 168.934	70 Yb Ytterbium 173.04	71 Lu Lutetium 174.967
Actinide Series	89 Ac Actinium 227.028	90 Th Thorium 232.038	91 Pa Protactinium 231.036	92 U Uranium 238.029	93 Np Neptunium 237.048	94 Pu Plutonium 244.064	95 Am Americium 243.061	96 Cm Curium 247.070	97 Bk Berkelium 247.070	98 Cf Californium 251.080	99 Es Einsteinium [254]	100 Fm Fermium 257.095	101 Md Mendelevium 258.1	102 No Nobelium 259.101	103 Lr Lawrencium [262]

Alkali Metal | Alkaline Earth | Transition Metal | Semimetal | Nonmetal | Basic Metal | Halogen | Noble Gas | Lanthanide | Actinide

TWOJE pismo o nauce

KAMELEONIZM WŚRÓD GWIAZD

ZASKAKUJĄCE SKŁADNIKI PERFUM

ARCHITEKCI RATUJĄ ŚWIAT

WIEDZA I ŻYCIE

MARZEC 2017 nr 3 (987)
CENA 7,99 zł (w tym 8% VAT)
www.wiz.pl
ukazuje się od 1926 roku

IN VITRO PRZYSZŁOŚCI

Kosmiczne FARMY

INTERNETOWY instynkt stadny

RADON wszechobecny zabójca

PRÓSZYŃSKI MEDIA

PRZYDATNE W SZKOLE

PUSTYNNY ZAMEK HERODA

Journal of chemical & engineering data

Article

pubs.acs.org/jced

Prediction of Radon-222 Phase Behavior by Monte Carlo Simulation

Jason R. Mick, Mohammad Soroush Barhaghi, and Jeffrey J. Potoff*

J. Chem. Eng. Data 2016, 61, 1625−1631

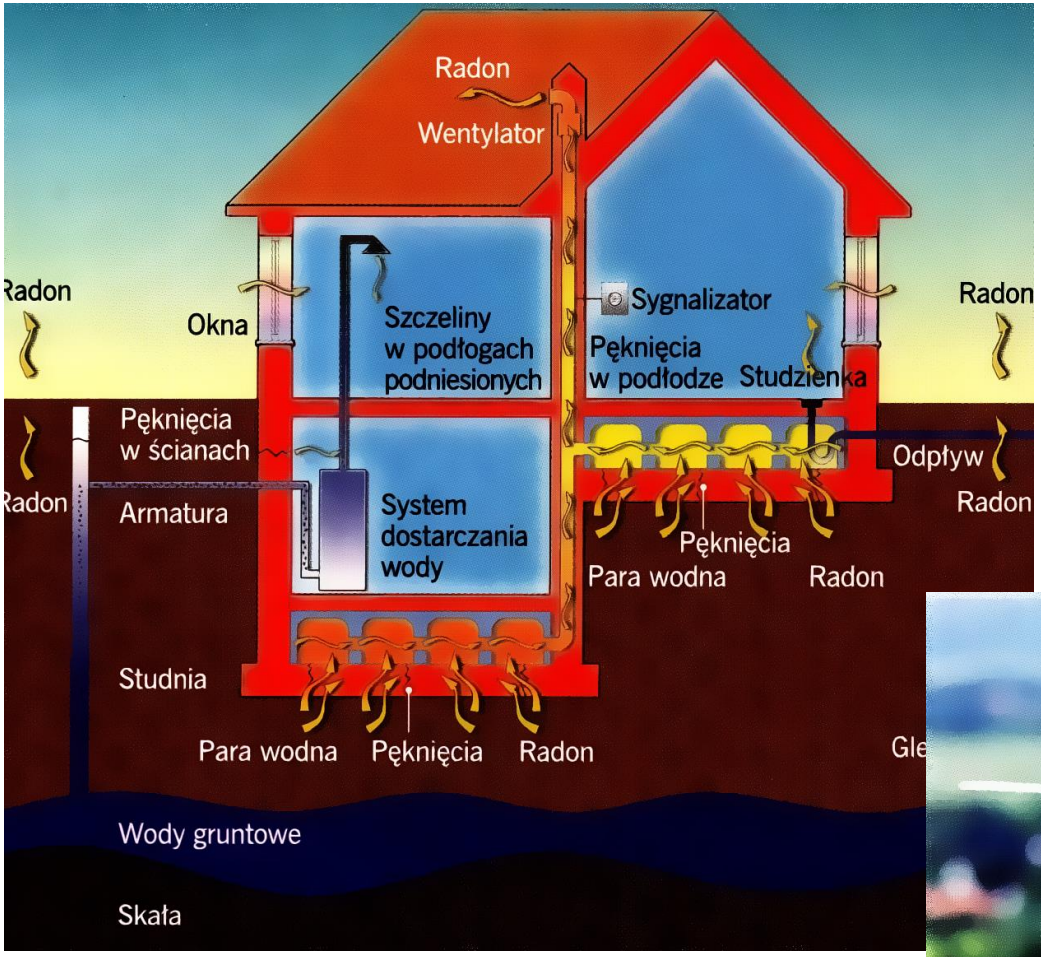
Radon
Wentylator
Radon
Okna
Szczeliny
w podłogach
podniesionych
Sygnalizator
Pęknięcia
w podłodze
Studzienka
Radon
Pęknięcia
w ścianach
Radon
Armatura
System
dostarczania
wody
Odpływ
Radon
Pęknięcia
Para wodna
Radon
Studnia
Para wodna
Pęknięcia
Radon
Wody gruntowe
Skała


UMWELTÜBERWACHUNG – LUF
MP-NR. 63.30

Virtual Porous Carbons (VPCs)

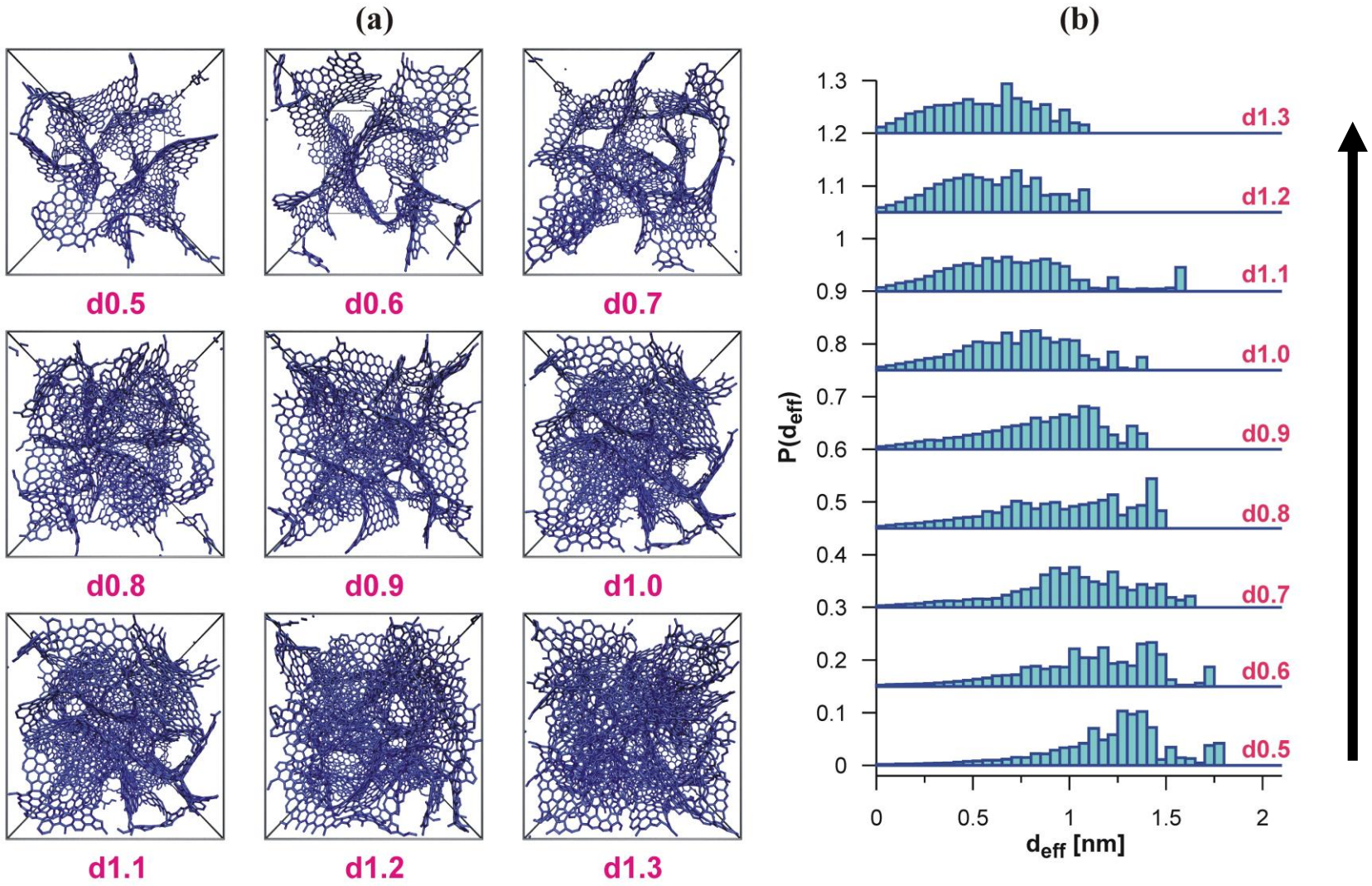

[S. Furmaniak, *Comput. Methods Sci. Technol.* 19 (2013) 47]

Ar, 87 K

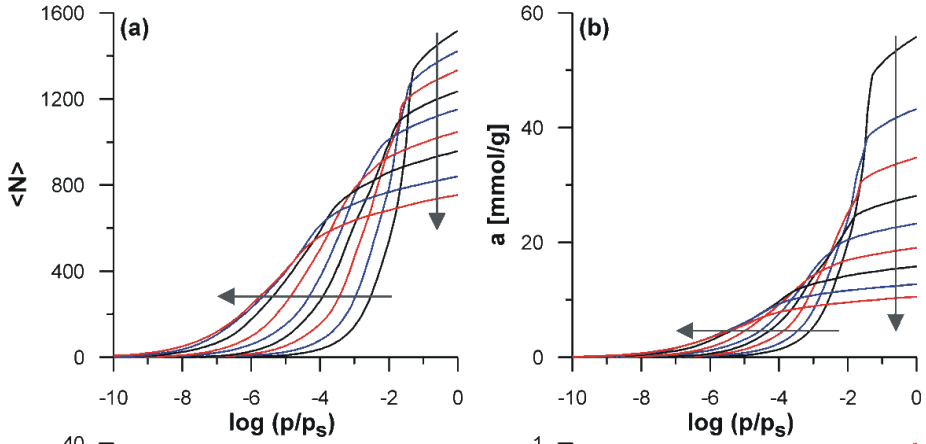
(a)
<N>
log (p/p$_s$)

(b)
a [mmol/g]
log (p/p$_s$)

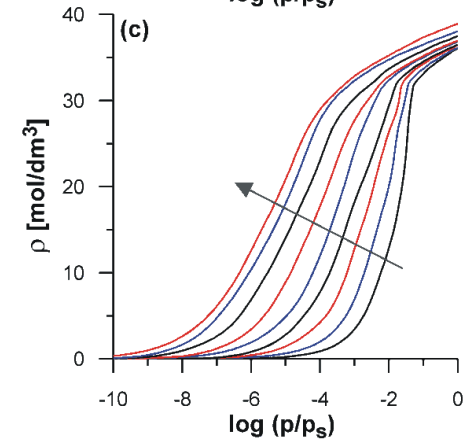
(c)
ρ [mol/dm^3]
log (p/p$_s$)

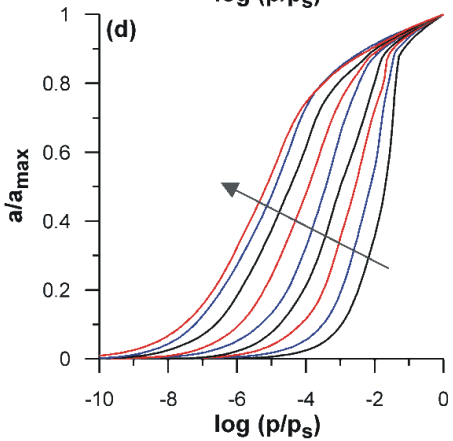
(d)
a/a$_{max}$
log (p/p$_s$)

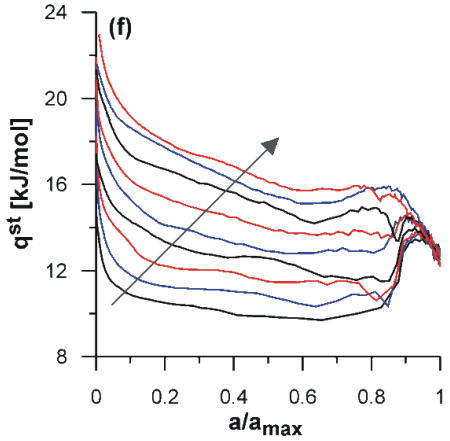
(f)
qst [kJ/mol]
a/a$_{max}$

Ar, 87 K

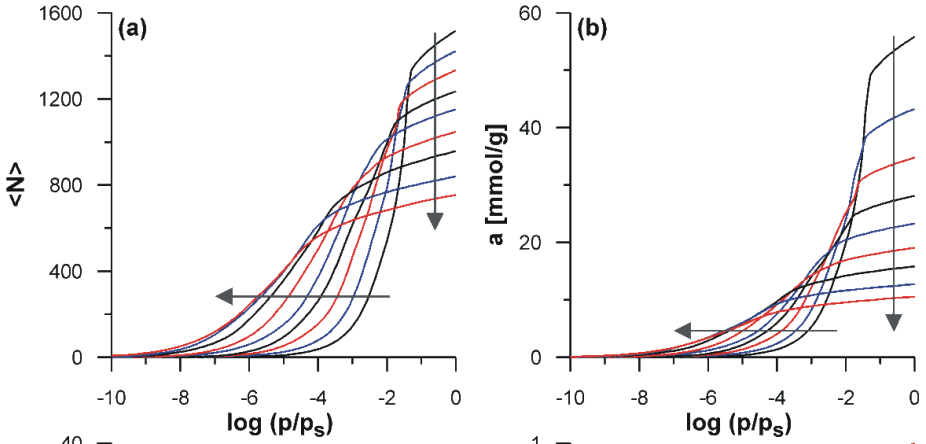
(a)
<N>
log (p/p$_s$)

(b)
a [mmol/g]
log (p/p$_s$)

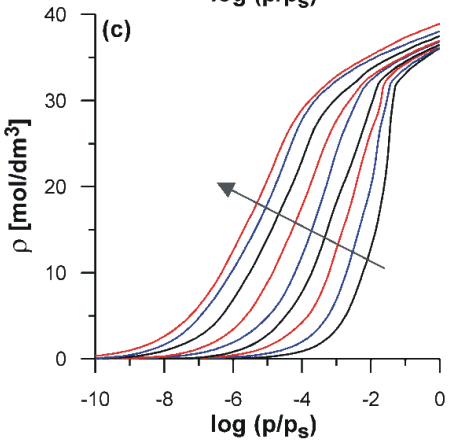
(c)
ρ [mol/dm^3]
log (p/p$_s$)

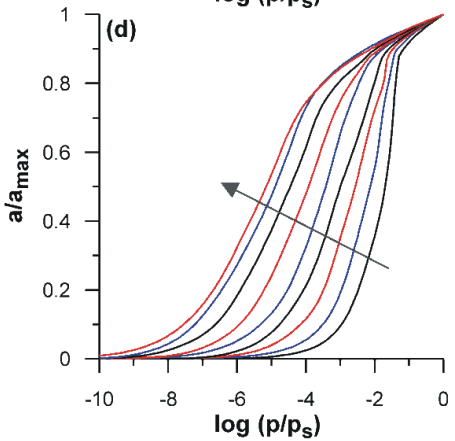
(d)
a/a$_{max}$
log (p/p$_s$)

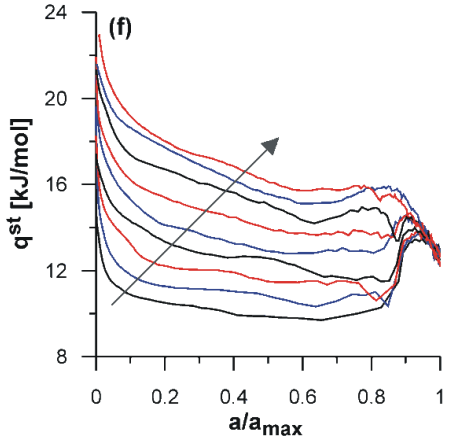
(f)
qst [kJ/mol]
a/a$_{max}$

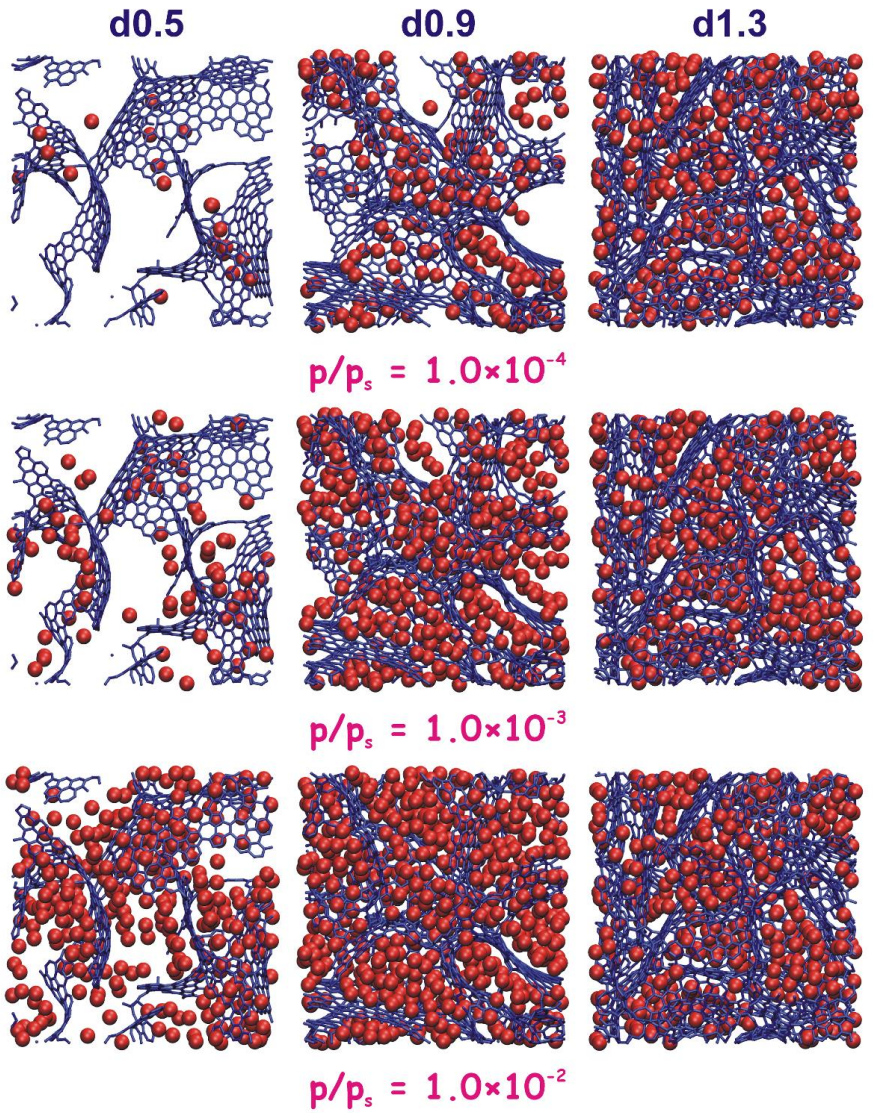
d0.5
d0.9
d1.3
p/p$_s$ = 1.0×10^{-4}
p/p$_s$ = 1.0×10^{-3}
p/p$_s$ = 1.0×10^{-2}

Rn, 298 K

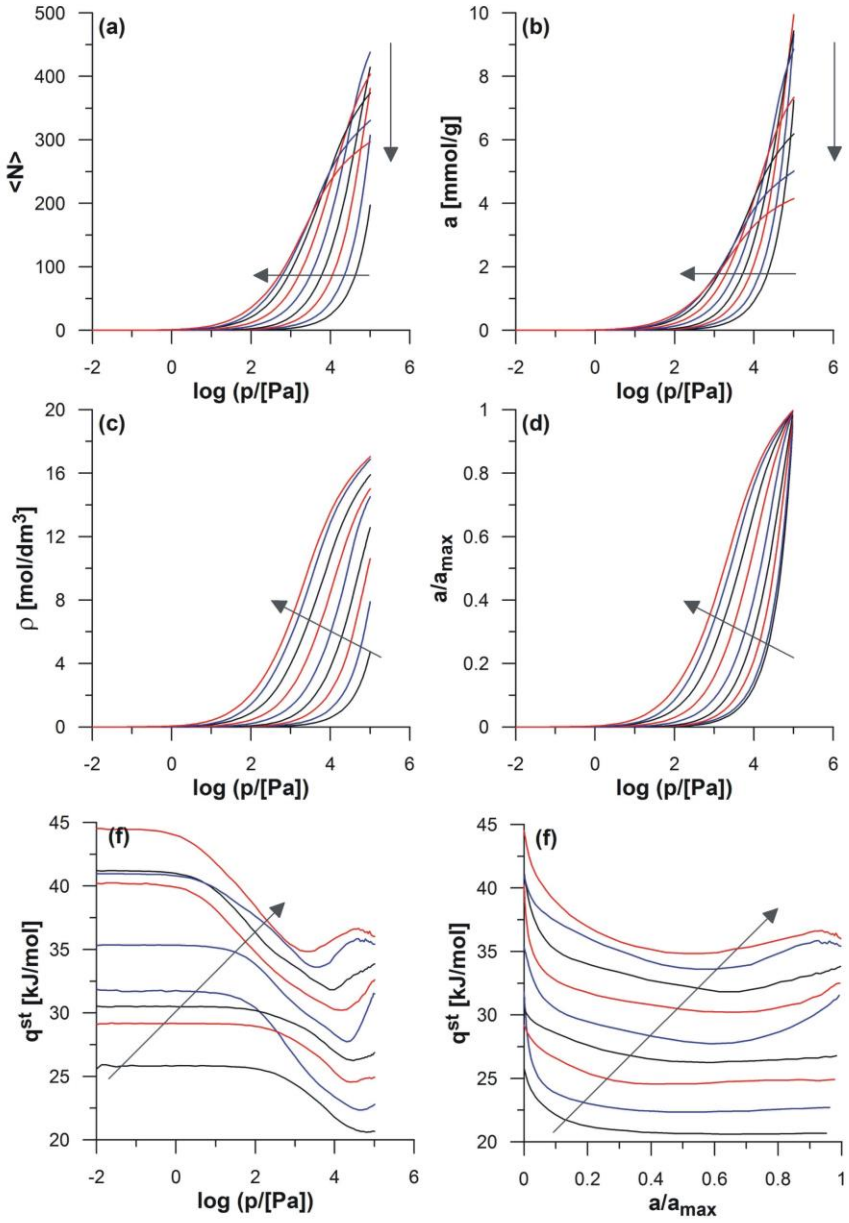
(a)
<N>
log (p/[Pa])
(b)
a [mmol/g]
log (p/[Pa])
(c)
ρ [mol/dm³]
log (p/[Pa])
(d)
a/a_max
log (p/[Pa])
(f)
q^st [kJ/mol]
log (p/[Pa])
(f)
q^st [kJ/mol]
a/a_max

Rn, 298 K

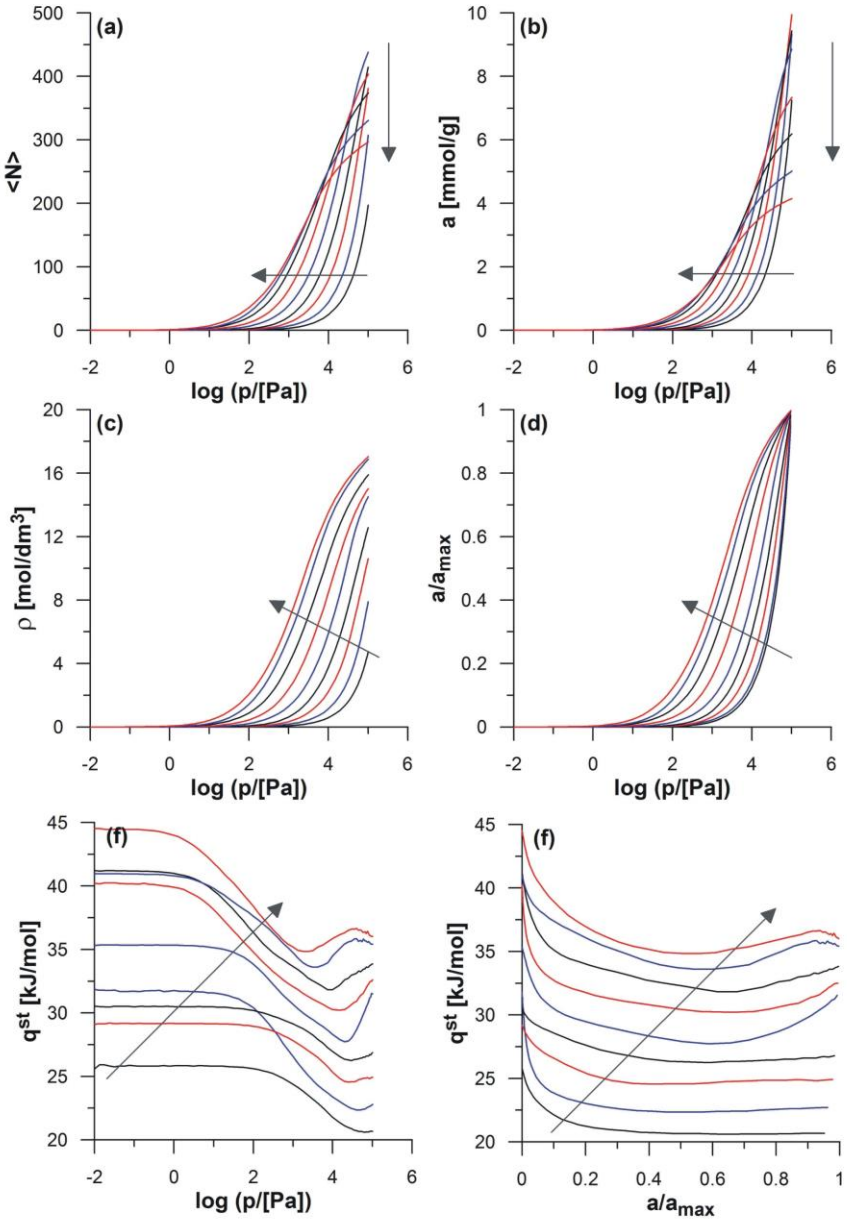
(a)
<N>
log (p/[Pa])
(b)
a [mmol/g]
log (p/[Pa])
(c)
ρ [mol/dm³]
log (p/[Pa])
(d)
a/a_max
log (p/[Pa])
(f)
q^st [kJ/mol]
log (p/[Pa])
(f)
q^st [kJ/mol]
a/a_max

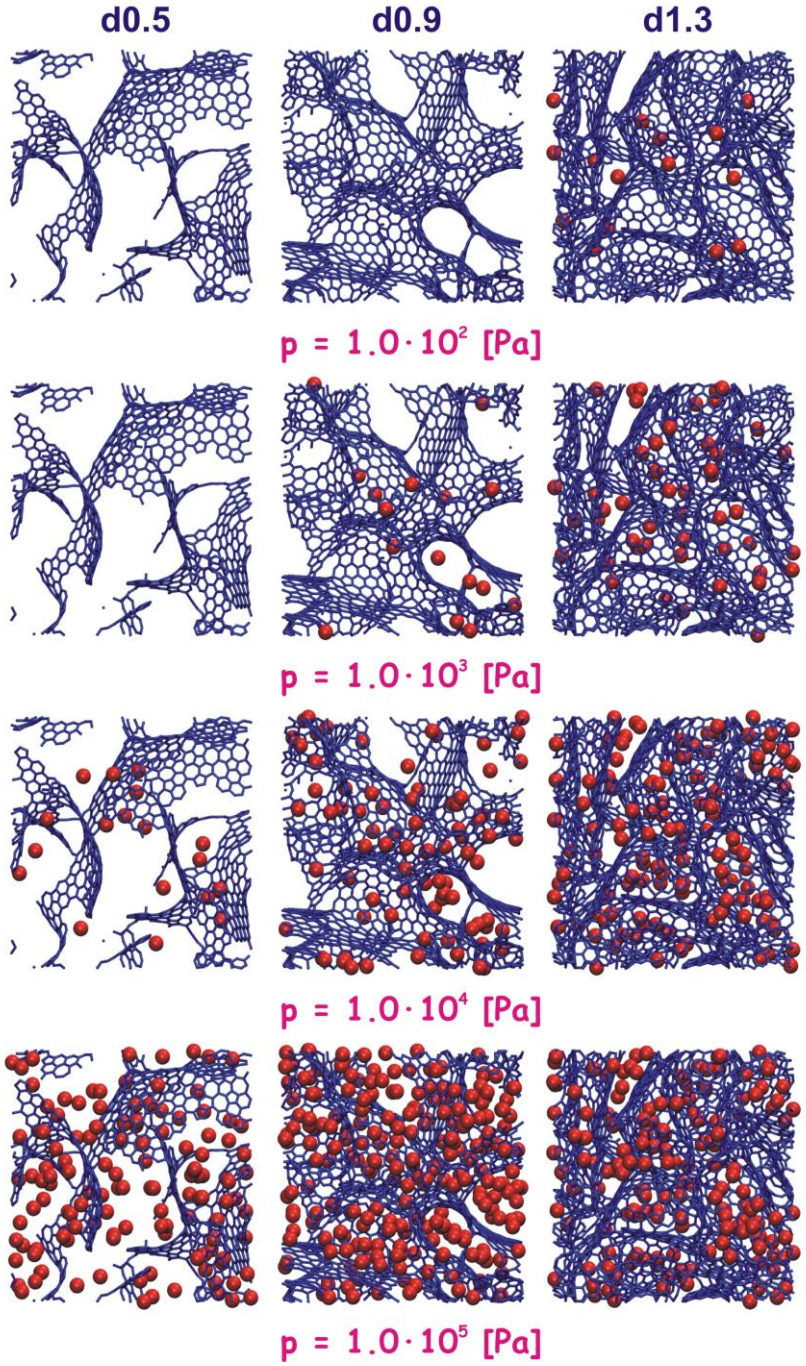
d0.5
d0.9
d1.3
p = 1.0·10² [Pa]
p = 1.0·10³ [Pa]
p = 1.0·10⁴ [Pa]
p = 1.0·10⁵ [Pa]

Thank you